Molecular Characterization of Caveolin Association with the Golgi Complex: Identification of a Cis-Golgi Targeting Domain in the Caveolin Molecule

Robert Luetterforst,* Espen Stang,* Natasha Zorzi,* Amanda Carozzi,* Michael Way,‡ and Robert G. Parton*

*Centre for Microscopy and Microanalysis, Department of Physiology and Pharmacology, and Centre for Molecular and Cellular Biology, University of Queensland, Brisbane, Queensland 4072, Australia; and ‡European Molecular Biology Laboratory, 69012 Heidelberg, Germany

Abstract. Caveolins are integral membrane proteins which are a major component of caveolae. In addition, caveolins have been proposed to cycle between intracellular compartments and the cell surface but the exact trafficking route and targeting information in the caveolin molecule have not been defined. We show that antibodies against the caveolin scaffolding domain or against the COOH terminus of caveolin-1 show a striking specificity for the Golgi pool of caveolin and do not recognize surface caveolin by immunofluorescence. To analyze the Golgi targeting of caveolin in more detail, caveolin mutants were expressed in fibroblasts. Specific mutants lacking the NH_2 terminus were targeted to the cis Golgi but were not detectable in surface caveolae. Moreover, a 32–amino acid segment of the putative COOH-terminal cytoplasmic domain of caveolin-3 was targeted specifically and exclusively to the Golgi complex and could target a soluble heterologous protein, green fluorescent protein, to this compartment. Palmitoylation-deficient COOH-terminal mutants showed negligible association with the Golgi complex. This study defines unique Golgi targeting information in the caveolin molecule and identifies the cis Golgi complex as an intermediate compartment on the caveolin cycling pathway.

Key words: caveolae • caveolin • Golgi complex • targeting • palmitoylation

Caveolae are a characteristic plasma membrane feature of many mammalian cell types. Since their first visualization by the pioneers of electron microscopy (Palade, 1953; Yamada, 1955), caveolae have been defined by their characteristic morphology appearing as bulb-shaped uncoated invaginations of 55–80nm diameter (Severs, 1988; Anderson, 1993, 1998; Parton, 1996). They are the major surface feature of many highly differentiated mammalian cells such as adipocytes, smooth muscle cells, and endothelial cells. In the latter, caveolae have been shown to bud from the surface and transport solutes across the endothelial monolayer (Simionescu and Simionescu, 1991; Schnitzer et al., 1994). In fibroblasts caveolae have been proposed to represent an alternative endocytic pathway (Montesano et al., 1982; Tran et al., 1987; Parton et al., 1994) and recent evidence suggests caveolae are vehicles for the entry of certain viruses into animal cells (Anderson et al., 1996; Stang et al., 1997; Parton and Lindsay, 1999).

A significant advance in the caveolae field came with the cloning and characterization of caveolins (VIP21/caveolin-1, caveolin-2, and caveolin-3 [cav-1, -2, -3])[1], major membrane proteins of caveolae (Glenney and Soppet, 1992; Kurzchalia et al., 1992; Way and Parton, 1995; Scherer et al., 1996; Tang et al., 1996). Caveolins are integral membrane components which form a hairpin in the membrane with both NH_2 and COOH termini oriented towards the cytoplasm (Dupree et al., 1993; Monier et al., 1995). Caveolins share a putative 33–amino acid intramembrane domain flanked by charged residues. Recent evidence suggests that caveolins are structural components involved in caveolae formation (Parton, 1996), key regulators of signaling events (Okamoto et al., 1998) and involved in cholesterol transport and regulation (Fielding

Dr. Espen Stang's present address is Institute of Pathology, The National Hospital, Oslo, Norway.

Address correspondence to Dr. R.G. Parton, Centre for Microscopy and Microanalysis, University of Queensland, Brisbane, Queensland 4072, Australia. Tel.: 61-7-3365-6468. Fax: 61-7-3365-4422. E-mail: r.parton@mailbox.uq.oz.au

1. *Abbreviations used in this paper*: cav-1, -2, -3, caveolin-1, -2, -3; GFP, green fluorescent protein; SFV, Semliki Forest Virus; WT, wild-type.

Published June 28, 1999

and Fielding, 1997). Expression of cav-1 in cells that lack caveolae causes de novo formation of caveolae (Fra et al., 1995b; Lipardi et al., 1998). This property may be dependent on the self-association of caveolin to form oligomers (Monier et al., 1995; Sargiacomo et al., 1995) and interaction with both cholesterol (Murata et al., 1995) and glycosphingolipids (Fra et al., 1995a) in detergent-insoluble glycosphingolipid-enriched surface domains (DIGs; Parton and Simons, 1995). We have also postulated that this property has been exploited in the formation of other cell surface domains such as the T-tubule system of muscle cells (Parton et al., 1997).

Accumulating evidence in vitro and in vivo suggests a key role for caveolins in signal transduction. Caveolins show a functional interaction with the small GTP binding protein ras (Song et al., 1996), src kinases (Li et al., 1996b), trimeric G protein subunits (Li et al., 1995), and other signaling molecules (reviewed by Okamoto et al., 1998). It has been proposed that caveolin oligomers may form a scaffold upon which signaling molecules are sequestered on the cytoplasmic side of the plasma membrane. Despite these advances, the relationship of the highly conserved structure of caveolae to their role in signaling remains unclear and some cell types are apparently able to mediate signaling events without invaginated caveolae or caveolins (Fra et al., 1994; Gorodinsky and Harris, 1995).

The majority of the above studies have concentrated on the plasma membrane role of caveolins, yet there is considerable evidence for a functional role of caveolin in intracellular compartments. In particular, caveolins have been implicated in polarized vesicular traffic in epithelia (Scheiffele et al., 1998) and in cholesterol transport (Smart et al., 1994, 1996; Fielding and Fielding, 1997). Both of these functions appear to rely on a dynamic cycling of caveolin through the cell. Antibodies to the NH_2 terminus of cav-1 preferentially label surface caveolae (Dupree et al., 1993) but antibodies against the COOH terminus of the same protein show a staining pattern characteristic of the Golgi complex (Dupree et al., 1993). This pattern was interpreted as representing the TGN on the basis of colocalization of caveolin with a viral protein accumulated in the TGN at 20°C by confocal microscopy. These observations, together with the identification of cav-1 within post TGN vesicles (Kurzchalia et al., 1992), suggested that cav-1 constantly cycles between the TGN and the cell surface (Dupree et al., 1993). Recent work showed that antibodies to cav-1 specifically inhibit transport from the TGN to the apical surface (Scheiffele et al., 1998). These results, together with studies showing a role for cholesterol in apical transport (Keller and Simons, 1998), have led to a model in which caveolin plays a role in the formation or stabilization of lipid domains within the TGN (Simons and Ikonen, 1997). This model relies on rapid trafficking of caveolin between the surface and the TGN. Other data provided evidence for a less conventional cycling pathway for cav-1. These studies showed that cav-1 redistributes to the lumen of the ER in response to treatment with cholesterol oxidase in a reversible manner (Smart et al., 1994). This cycle appears to occur constitutively even without cholesterol oxidase treatment and can be disrupted by treatment with microtubule-depolymerizing agents when caveolin accumulates within the endoplasmic reticulum/Golgi intermediate compartment (ERGIC; Conrad et al., 1995). This pathway was proposed to play a role in cholesterol transport; caveolin directly binds cholesterol (Murata et al., 1995) and caveolin expression increases cholesterol transport from the ER to the plasma membrane (Smart et al., 1996) apparently via a cytosolic intermediate (Uittenbogaard et al., 1998). As cav-1 expression is regulated by cholesterol (Fielding et al., 1997; Hailstones et al., 1998) through cholesterol-responsive promoter elements (Bist et al., 1997) this points to a primary role for caveolin in cholesterol homeostasis.

In view of these apparently conflicting data, we have reassessed and further characterized the intracellular location and routing of caveolin using immunofluorescence and immunoelectron microscopy and a mutational approach. We show that antibodies to the COOH terminus of cav-1 or to the scaffolding domain preferentially label caveolin within the cis-Golgi and not the cell surface. Golgi targeting information is located within the COOH terminus of the caveolin molecule and this domain is sufficient to target a soluble protein to the cytoplasmic face of the Golgi apparatus.

Materials and Methods

Materials

Polyclonal antibodies were raised against a peptide corresponding to a highly conserved region of cav-3, with a COOH-terminal cysteine for coupling to the carrier (CGFEDVIAEPEGTYSFDE). Antibodies were affinity purified as described previously (Parton et al., 1997). Other domain-specific caveolin anti-peptide antibodies have been described previously (Dupree et al., 1993). Anti-chick caveolin (anti-cavFL) was purchased from Zymed Laboratories. Affinity-purified rabbit antibodies (unconjugated and biotinylated) against p23 (Rojo et al., 1997) were provided by Dr. Manuel Rojo (University of Geneva, Switzerland). Antibodies against the mammalian KDEL-receptor ERD2 (Griffiths et al., 1994) and giantin (Linstedt and Hauri, 1993) were gifts of Dr. Hans-Peter Hauri (Biozentrum, Basel, Switzerland) and Dr. Hans-Dieter Soeling (Goettingen, Germany). Fluorescein-labeled anti–mouse IgG, Cy3-labeled anti–rabbit IgG and Cy2-labeled streptavidin were from Jackson ImmunoResearch. The hybridoma used to generate monoclonal mouse anti-HA was provided by Professor David James (University of Queensland). The rabbit anti-HA and the cDNA for myc-tagged sialotransferase were both kindly provided by Dr. Tommy Nilsson (EMBL, Heidelberg, Germany). Nocodazole was purchased from Sigma Chemical Co. and was kept at −20°C (stock solution 10 mM in DMSO).

Cell Culture

BHK cells were grown and maintained as described previously (Gruenberg et al., 1989). Primary human fibroblasts were a gift of Professor D. James and were maintained in RPMI supplemented with 10% FCS. C2C12 cells were cultured as described previously (Way and Parton, 1995).

Recombinant Semliki Forest Virus

Recombinant Semliki Forest Virus (SFV)-cav-1 and SFV-cav-3 were prepared in BHK cells according to an established protocol (Liljestrom and Garoff, 1991; Olkkonen et al., 1993). In brief, canine cav-1 and mouse cav-3 were PCR amplified from the original clones with introduced 5′ BamHI and 3′ SmaI restriction sites. After sequencing of both strands, the cDNAs were cloned into the appropriate sites of pSFV1 (Gibco, Grand Island, NY). RNA was generated by in vitro transcription from pSFV-cav-1, pSFV-cav-3, and pSFV-Helper1 and electroporated into BHK cells. Culture supernatant was harvested after 48 h and frozen at −70°C. The BHK cells used to produce recombinant SFV were harvested and prepared for Western blotting. The expression level of cav-1 was >10-fold higher than endogenous levels.

Published June 28, 1999

For immunofluorescence experiments cells were infected with undiluted recombinant SFV containing culture supernatant for 1 h at 37°C after which the infection medium was diluted 10-fold with normal culture medium and incubated for a further 12 h. The cav-2-SFV construct was kindly provided by Dr. Elina Ikonen (National Public Health Institute, Helsinki, Finland).

Subcellular Fractionation

BHK cell fractions were kindly provided by Professor Jean Gruenberg. BHK cells were homogenized in isotonic sucrose solution and the membranes of the post-nuclear supernatant were fractionated using a step sucrose gradient to produce a fraction enriched in p23 and ERD2 exactly as described (Rojo et al., 1997).

Cloning and Expression

A series of NH_2-terminal truncation mutants of cav-3 were generated from the original cDNA clone by PCR. $Cav3^{DIH}$ (residues 16-151), $Cav3^{NED}$ (residues 33–151), $Cav3^{DGV}$ (residues 54–151), and $Cav3^{KSY}$ (residues 108–151) were generated using the forward primers DIHfor 5′ CGGGGTACCACCATGGACATTCACTGCAAGGAG 3′, NEDfor 5′ CGGGGTACCATGAATGAGGACATTGTGAAG 3′, DGVfor 5′ CGGGGTACCACCATGGACGGTGTATGGAAGGTG 3′ and KSYfor 5′ CGGGGTACCACCATGAAGAGCTACCTGATCGAG 3′, respectively, and the reverse primer RORrev 5′ CCGGAATTCTTAGCCTTCCCTTCGCAGCACCACCTT 3′. Similarly, truncations of cav-1 (residues 135–183) were generated with and without three putative COOH-terminal palmitoylation site cysteines mutated to alanine. Wild-type (WT) cav-1 cDNA template was used to generate $Cav1^{KSF}$ and cav-1 (Cys-Ala) cDNA template was used to generate $Cav1^{KSF}\Delta p$ both using the forward primer CAV1(KSF)for 5′ CGGGGTACCACCATGAAGAGTTTCCTGATTGAGATTCAGTGC 3′ and the reverse primer CAV1HArev 5′ ATAAGAATGCGGCCGCCTGTTTCTTTCTGCATGTTGATGCGG 3′. The resulting mutants were cloned into pCB6-KXHA (Way and Parton, 1995), a derivative of the eukaryotic expression vector pCB6, containing the HA epitope tag (YPYDVPDYA), downstream of an in frame NotI site.

The $Cav3^{KSY}$ region was also amplified with the forward primer, KSYGFPfor 5′ CCGGAATTCGAAGAGCTACCTGATCGAG 3′, and the reverse primer, CAV3rev 5′ TCCCCCCGGGTTAGCCTTCCCTTCGCAGCACC 3′, for in frame insertion into the COOH-terminal green fluorescent protein (GFP) fusion vector, pEGFP-C1 (CLONTECH Laboratories).

Further truncations of $Cav3^{KSY}$ were similarly prepared using the following combinations of primers; $Cav3^{IYS}$ (residues 120–151) and $Cav3^{IRT}$ (residues 125–151) used the forward primers, IYSfor 5′ GGAATTCCATCTACTCACTGTGTATCCGC 3′ and IRTfor 5′ GGAATTCCATCCGCACCTTCTGC 3′ respectively, with the reverse primer CAV3rev.

Cav-3ΔC, a COOH-terminal truncation mutant of cav-3 (residues 1–107) was generated using the forward primer, CAV3GFPfor 5′ CCGGAATTCAATGATGACCGAAGAGCACACGG 3′, and the reverse primer, CAVΔCrev 5′ TCCCCCGGGTTAAATGCAGGGCACCACGGC 3′. Full-length cav-3 was similarly produced using the forward primer, CAV3GFPfor, and the reverse primer, CAV3rev. The products were then cloned into pBluescript (Stratagene) and subcloned into pEGFP-C1. The sequences of all constructs were confirmed by sequencing of both strands in pBluescript using the T3 and T7 primers.

BHK, FRT, C2C12, and CV-1 cell lines were transiently transfected using Lipofectamine (GIBCO BRL) according to the manufacturer's instructions. In brief, cells were grown to ~50% confluence on coverslips and 10-cm dishes for immunofluorescence and electron microscopy, respectively, or 90% confluence on 10-cm dishes for biochemical analysis. The cells were washed twice with serum-free media before being transfected with a ratio of 1 μg DNA to 5 μl Lipofectamine per 1 ml of Opti-MEM (GIBCO BRL). The transfection mixture was left on the cells for 6 h before being washed with, and changed to, normal growth media lacking antibiotics and incubated for a further 18 h before fixation or harvesting. Nocodazole treatment was at a concentration of 10 μM for 2 h at 37°C before fixation.

Preparation of Crude Fractions

Confluent dishes of cells were washed twice with cold PBS before being scraped into ice-cold HES homogenization buffer (0.25 M sucrose, 1 mM EDTA, and 20 mM Hepes, pH 7.4) containing protease inhibitors. Cells were homogenized by passaging through a 27-G syringe and nuclei and unbroken cells were removed by centrifugation at 1,000 *g* for 5 min at 4°C. The resulting supernatant was then centrifuged at 100,000 *g* for 30 min at 4°C to separate cytosol (supernatant) from cellular membranes (pellet). For Western analysis the pellet was extracted with a volume of 1% SDS HES or 1% Triton X-100 HES equal to the volume of supernatant for 10 min at ambient temperature followed by centrifugation at 10,000 *g* for 5 min at to remove insoluble material. Similarly, salt extractions were performed on the pellet with volumes of 1 M KCl in 50 mM Tris, pH 8.0, or 0.1 M Na_2CO_3, pH 11.5, equal to the supernatant. Triton X-114 phase separation was achieved using the method of Bordier (1981), with the exception that membranes (100,000-*g* pellet) were resuspended in the initial solution.

Western Blotting

Equal volumes of cytosol (100,000-*g* supernatant) and the detergent extracted microsomal membranes (100,000-*g* pellet) were boiled in SDS PAGE sample buffer. After electrophoresis proteins were transferred to Immobilon membrane (Millipore Corp.) using a Bio Rad trans blot semidry transfer cell. Membranes were blocked with 5% nonfat dry milk TBS-T (0.15 M NaCl, 0.1% Tween 20, and 20 mM Tris, pH 7.4) followed by incubation in specific antibody diluted in 1% nonfat dry milk TBS-T. After washing with TBS-T membranes were incubated with a second antibody diluted in 0.2% BSA TBS-T. Bound antibody was detected using the enhanced chemiluminescence detection system (Amersham Corp.).

Immunofluorescence Microscopy

Cells were grown on glass coverslips and fixed with either methanol (−20°C, ≥5 min) or 3% paraformaldehyde (PFA, 20°C, ≥20 min). PFA-fixed cells were permeabilized for 5 min with 0.1% (wt/vol) saponin in PBS and labeled as described previously (Parton et al., 1997). For double labeling with mouse and rabbit antibodies, cells were incubated with the mixture of primary antibodies for 30 min, washed three times with PBS, and incubated with a mixture of fluorescein- or Cy3-labeled anti–mouse IgG and Cy3- or fluorescein-labeled anti–rabbit IgG for 20 min. In some experiments, cells were double labeled with two rabbit antibodies (p23 and anti-concav). This was perfomed using the following sequence: anti-concav, Cy3 goat anti–rabbit, a blocking irrelevant rabbit antibody (anti-cholera toxin), then biotinylated rabbit anti-p23 followed by streptavidin-Cy2 (Monarch Medical). Control experiments omitting the primary antibodies showed the specificity of the labeling. Samples were analyzed with a confocal laser scanning microscope (Bio Rad Laboratories) equipped with an argon and a helium/neon laser for double fluorescence at 488 and 543 nm. Fluorescein/Cy2 and Cy3 signals were recorded sequentially (emission filters: BP510-525 and LP590) using 63 or 100× plan-APOCHROMAT oil immersion objectives. For overlay, fluorescein and Cy3 images were adjusted to similar output intensities and merged with Adobe Photoshop 3.0.5 into a composite RGB image using a Power Macintosh 7500/100 computer. Figures were arranged with Microsoft PowerPoint.

Colocalization was quantitated by analysis of confocal images of double-labeled nocodazole-treated cells in which individual puncta were clearly evident (e.g., see Fig. 4). Images were digitally captured and overlaid using the RGB function of Adobe Photoshop. Separate images were adjusted to equivalent intensities. IP Lab Spectrum software was then used to analyze the images for the area occupied by the colocalizing elements as a percentage of the total labeled area. Results are expressed as the mean of five fields ± SEM. Note that this technique allows a comparison of the degree of overlap of different markers but underestimates the actual puncta which are positive for both markers (e.g., cav/p23 showed a 63% colocalization but >90% of puncta were labeled for both markers; see for example Fig. 4).

Electron Microscopy

Cells were fixed with 8% paraformaldehyde in 100 mM phosphate buffer, pH 7.35, or with the same fixative containing 0.1% glutaraldehyde for 30 min at RT and then processed for frozen sectioning as described previously (Parton et al., 1997). BSA-gold was internalized as a fluid phase marker for 10 min or 30 min at 37°C as described previously (Kobayashi et al., 1998).

Published June 28, 1999

Results

Localization of Expressed Epitope-tagged Cav-1 and Cav-3, and Endogenous Cav-1 in Cultured Cells

We have previously shown that cav-1 is localized to the Golgi complex and to surface caveolae when expressed in BHK cells (Dupree et al., 1993). We investigated the use of a transfection approach to express caveolin mutants to study caveolin targeting. As caveolin can form homo-oligomers which could potentially influence the distribution of introduced caveolins, we investigated the use of cav-3 to study caveolin targeting as BHK cells lack endogenous cav-3. Previous work using GST-fusion proteins of caveolin has shown that cav-1FL or COOH- or NH_2-terminal truncation mutants can oligomerize with full-length cav-1 but not cav-3 (Song et al., 1997). Also in vivo cav-1 is sorted away from cav-3 when expressed in differentiating muscle cells (Parton et al., 1997).

Epitope-tagged cav-1 and cav-3 were expressed in BHK cells. As shown in Fig. 1, A and B, cav-1 and cav-3 showed a similar distribution as judged using antibodies against a COOH-terminal epitope tag (VSV-G and HA, respectively). The proteins were localized to the cell surface and to a perinuclear compartment, assumed to represent the Golgi complex (Dupree et al., 1993; see below). A similar distribution was observed upon expression of a fusion protein comprising GFP fused to the NH_2 terminus of cav-3 (Fig. 1 C). These results suggest that heterologously expressed cav-1 and cav-3 localize to the same compartments in BHK cells and can be used to study caveolin targeting.

To further investigate the subcellular localization of caveolin, we examined the distribution of endogenous caveolin using a number of different antibodies and cell lines. Previous studies differ in their analysis of caveolin distribution; some studies have shown that caveolin is only present at the cell surface unless cells are subjected to experimental manipulations (Smart et al., 1994), whereas others have concluded that caveolins exist in Golgi complex–associated and surface pools at steady state (Dupree et al., 1993). BHK, Vero, and MDCK cell lines as well as primary human fibroblasts, which have been extensively studied by others (Smart et al., 1994), were labeled with antibodies to the NH_2 terminus of cav-1 (anti-cav1N) and antibodies to the COOH terminus (anti-cav1C). Similar labeling patterns were observed in all the cell types studied; surface staining by anti-cav1N (e.g., human fibroblasts, Fig. 1 D) and a striking Golgi-type staining with anti-cav1C antibodies (Fig. 1 E). This suggests that different epitopes are exposed at these two cellular locations.

To investigate this possibility further we studied the exposure of a domain of the molecule which has already been extensively studied in terms of interacting proteins, by raising antibodies against the scaffolding domain of the caveolin family. This domain is conserved between caveolins, thereby acting as a signature motif, and is also conserved in evolution (Tang et al., 1997). Antibodies were raised in rabbits against a scaffolding domain peptide corresponding to the sequence of cav-3 (see Materials and Methods) and affinity purified on the corresponding peptide column. By Western blotting the affinity-purified antibody (anti-concav) recognized a doublet of ~21 kD in BHK membranes (Fig. 2 A), a single band in undifferentiated C2C12 myoblast membranes, and a single <20-kD band in differentiating C2C12 myotubes (Fig. 2 B). The

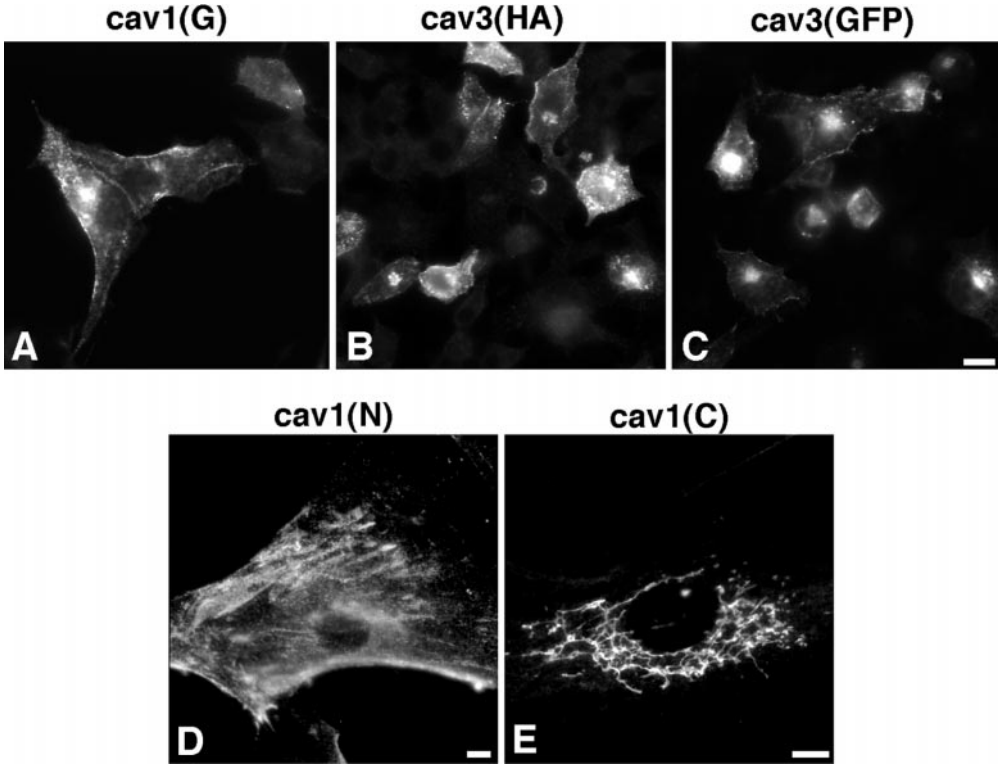

Figure 1. Localization of overexpressed epitope-tagged caveolins and endogenous cav-1 in BHK cells and fibroblasts. (A–C) BHK cells were transfected with VSV-G epitope-tagged cav-1 (cav1(G)), HA-tagged cav-3 (cav3(HA)), or with a fusion protein comprising GFP fused to the NH_2 terminus of cav-3 (cav3(GFP)) as indicated. The full-length caveolin constructs localize to the cell surface and perinuclear area. (D and E) Immunofluorescent detection of cav-1 in human fibroblasts. Cultured human fibroblasts were labeled with antibodies directed against either the NH_2 terminus or COOH terminus of cav-1 as indicated. Whereas the NH_2-terminal antibodies show a characteristic surface staining, antibodies against the COOH terminus show a Golgi-like staining pattern. Bars, 10 μm.

Published June 28, 1999

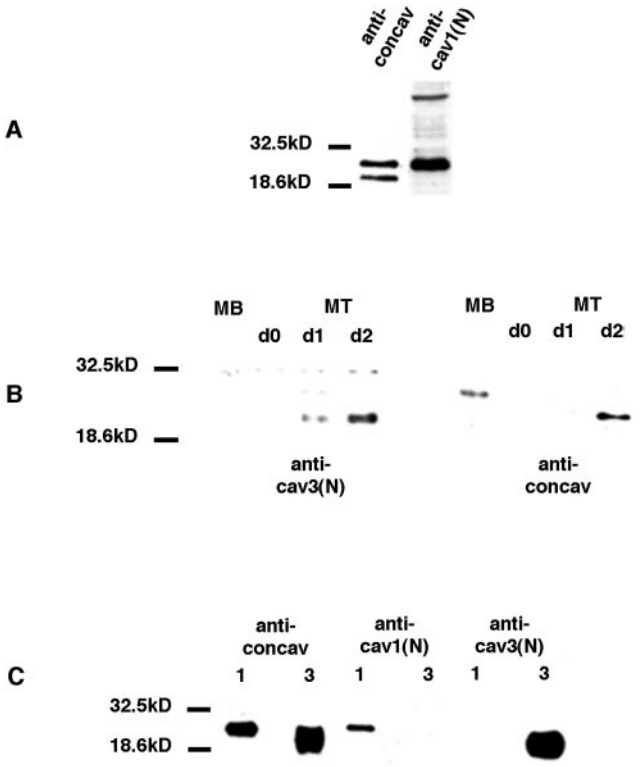

Figure 2. Characterization of an antibody to the conserved scaffolding domain of caveolins. Antibodies raised against either the conserved domain of cav-3 (anti-concav), the cav-1 NH_2 terminus (anti-cav1(N)), or the cav-3 NH_2 terminus (anti-cav3(N)) were used to blot BHK cell membranes (A), C2C12 myoblasts, and myotube membranes (B) or BHK cells overexpressing cav-1 or cav-3 (C). (A) The anti-concav antibody detects a doublet in BHK membranes, the upper band comigrating with the longer (α) form of cav-1 as shown with the anti-cav1(N) antibody. (B) Anti con-cav recognizes a ~21-kD band in undifferentiated C2C12 myoblasts (MB) and a <20-kD band in differentiating C2C12 myotubes (MT; B, d0, d1, and d2 indicate days of differentiation). The adjacent blot shows the same fractions probed with anti-cav3(N). (C) Cells expressing cav-1 (1) or cav-3 (3) were probed with the antibodies indicated. The anti-concav antibody recognizes both overexpressed cav-1 and cav-3.

signal was completely competed by the specific peptide to which it was raised (not shown). This suggested that the antibody (named anti-concav for consensus caveolin) recognized both cav-1 and cav-3, the predominant isoforms expressed in BHK cells and C2C12 myoblasts, and differentiating C2C12 myotubes, respectively. This was confirmed by blotting of BHK cells overexpressing cav-1 or cav-3 (Fig. 2 C). By immunofluorescence the antibody was shown to recognize overexpressed cav-1, cav-2, and cav-3 (Fig. 3, A–C) consistent with the predicted specificity.

The anti-concav gave a characteristic perinuclear staining on cell lines including BHK, CV-1, and MDCK (Fig. 3, D–F). Primary human fibroblasts revealed the same pattern of labeling which colocalized with the Golgi marker, p23 (Fig. 3, G–I). This staining pattern was distinct from that obtained with antibodies to the NH_2 terminus of cav-1, which as expected gave a surface staining pattern characteristic of caveolae (Fig. 1 D). This result suggested that the anti-concav antibody was unable to recognize surface caveolin. To test this possibility, we examined the staining pattern for anti-concav in differentiating C2C12 cells. In these cells cav-3 gives a characteristic staining pattern representing the surface-connected T-tubule system (Parton et al., 1997). The cav-3(N) antibody showed the characteristic reticular staining pattern as described previously (Parton et al., 1997) but the anti-concav showed no labeling of the T-tubules (results not shown). We then examined whether the strict specificity for intracellular caveolin was retained after overexpression, when interaction with surface molecules might be expected to be saturated. Even after high overexpression of cav-3 using the recombinant SFV expression system, the strict specificity of the concav antibody for the intracellular caveolin pool was still maintained with no sign of surface staining (compare Fig. 3 J, anti-cav-3(N) with Fig. 3 K, anti-concav). These experiments, in which antibody concentrations were optimized to allow only detection of overexpressed caveolin, also emphasize that the N- and concav antibodies were both recognizing the same heterologously expressed caveolin. In summary, the results suggest that the anti-concav and anti-cavC antibodies specifically recognize Golgi-associated caveolin and that changes in the accessibility or conformation of the epitope on transport of caveolin to the cell surface may inhibit antibody binding.

Antibodies to the COOH Terminus of Caveolin-1, to Concav, or to Purified Caveolin Localize to the Cis-Golgi Complex

In view of the different models for caveolin cycling, we sought to pinpoint the domain of the Golgi complex with which caveolin was associated. For this analysis we used a monoclonal commercial antibody against purified cav-1 (anti-cav1FL; see Fig. 4 A) together with either a cis-Golgi marker p23 (Rojo et al., 1997) or a TGN marker (transfected sialotransferase, tST; Rabouille et al., 1995). We found that cav-1 immunolabeling colocalized with the TGN marker tST in control cells as judged by confocal microscopy, consistent with previous studies; (Dupree et al., 1993), but the same high degree of colocalization was found with p23 (not shown). Therefore, we employed the microtubule-depolymerizing agent, nocodazole, which has been shown to disrupt the Golgi complex (Kreis, 1990) and has been used to localize proteins to distinct Golgi sub-compartments (e.g., Chavrier et al., 1990; Ullrich et al., 1996). Nocodazole treatment caused dispersion of Golgi markers into discrete puncta (Fig. 4). Double labeling of nocodazole-treated cells with cis- (p23) and trans-Golgi (tST) markers showed clear, although incomplete, segregation of the two markers (Fig. 4 B; note that many of the puncta are only labeled for one of the markers). After nocodazole treatment anti-cav1FL showed a relatively low degree of colocalization with tST (Fig. 4 D) but almost complete colocalization with p23 (see Fig. 4 C; virtually all p23 puncta are caveolin-positive). The level of colocalization was also quantitated as the area occupied by the colocalizing elements in the image as a percentage of the total labeled elements (see Materials and Methods for details). Consistent with the qualitative data, these results showed

Published June 28, 1999

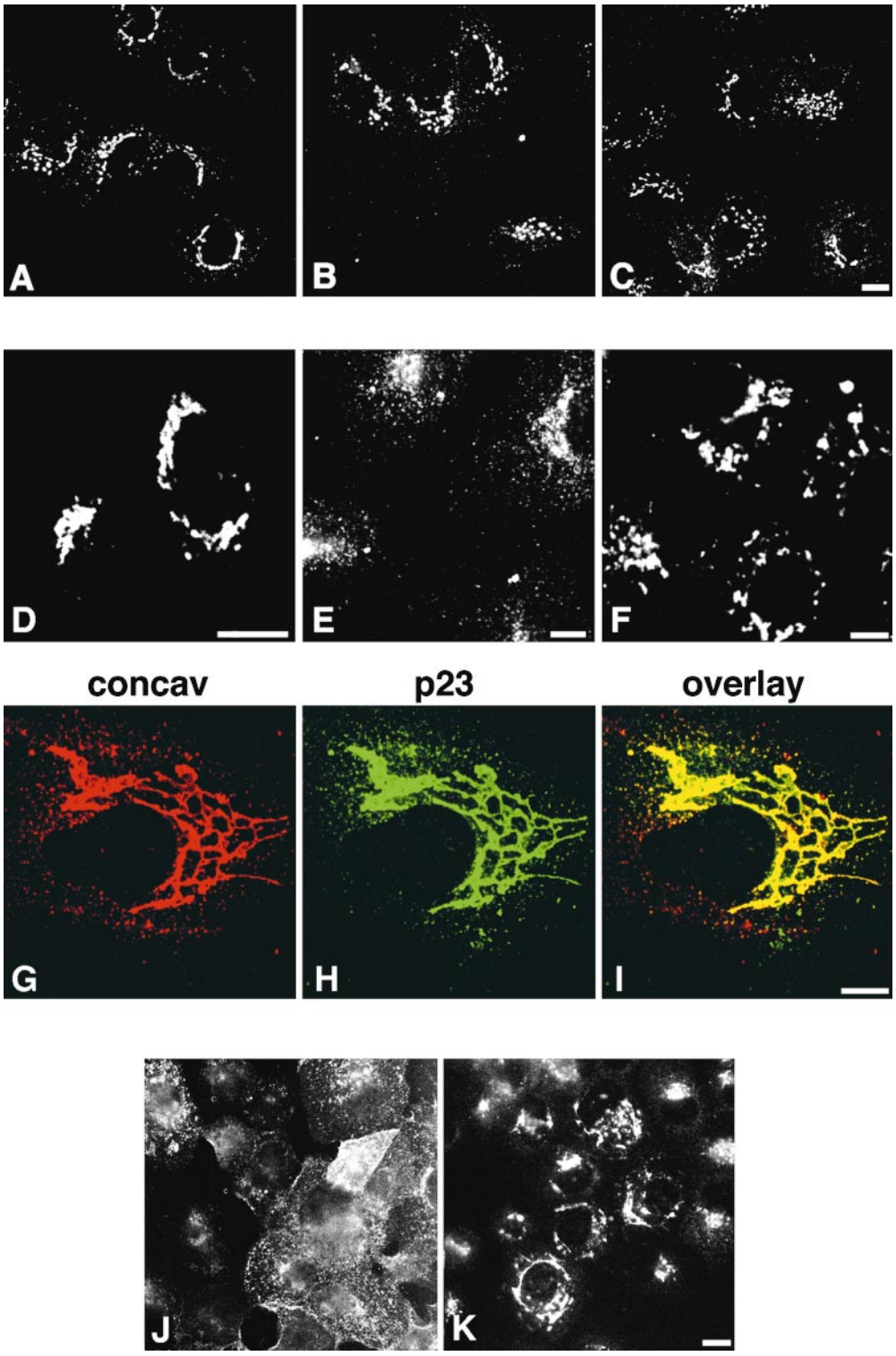

Figure 3. Immunofluorescence detection of caveolin using the anti-concav antibody. (A–C) FRT cells were infected with recombinant Semliki Forest Virus expressing cav-1 (A), cav-2 (B), or cav-3 (C). The cells were then labeled with affinity purified anti-concav antibodies and examined by confocal microscopy. The antibody recognizes all three caveolins by immunofluorescence. (D–F) A number of cell types were labeled with the anti-concav antibody as follows; BHK (D), CV-1 (E), MDCK (F), and primary human fibroblasts (G–I). In each case labeling is only detectable in the perinuclear area of the cell consistent with a Golgi localization pattern. This was confirmed by double labeling with a cis-Golgi marker, p23 in the human fibroblasts (H and I). (J and K) Immunofluorescence detection of overexpressed caveolin-3 with anti-cav3(N) and anti-concav antibodies. BHK cells were infected with recombinant SFV to express cav-3. The cells were then fixed and labeled with anti-cav3(N) antibodies (J) and anti-concav antibodies (K) and examined by confocal microscopy. Note the dramatic difference in the labeling patterns; surface and possible internal staining in J but only Golgi staining in K. Bars, 10 μm.

a much higher degree of colocalization for caveolin/p23 (63 ± 4%) than for caveolin/tST (46 ± 6%) or p23/tST (41 ± 4%). This suggests caveolin is present in the early Golgi and is not exclusively present in the TGN.

The subcellular location was further analyzed by immunoelectron microscopy. All the available antibodies gave low labeling of the Golgi complex on ultrathin frozen sections of intact cells. However, in frozen sections of BHK cell fractions enriched for p23 and ERD2 (Rojo et al., 1997), anti-cavC labeling colocalized with p23 on Golgi cisternae (Fig. 5). The higher labeling in this preparation presumably reflects greater accessibility of cytosolic epitopes as described for other Golgi proteins (Griffiths et al., 1994). Taken together the results show that under steady state conditions caveolin is detectable within the cis-Golgi.

Published June 28, 1999

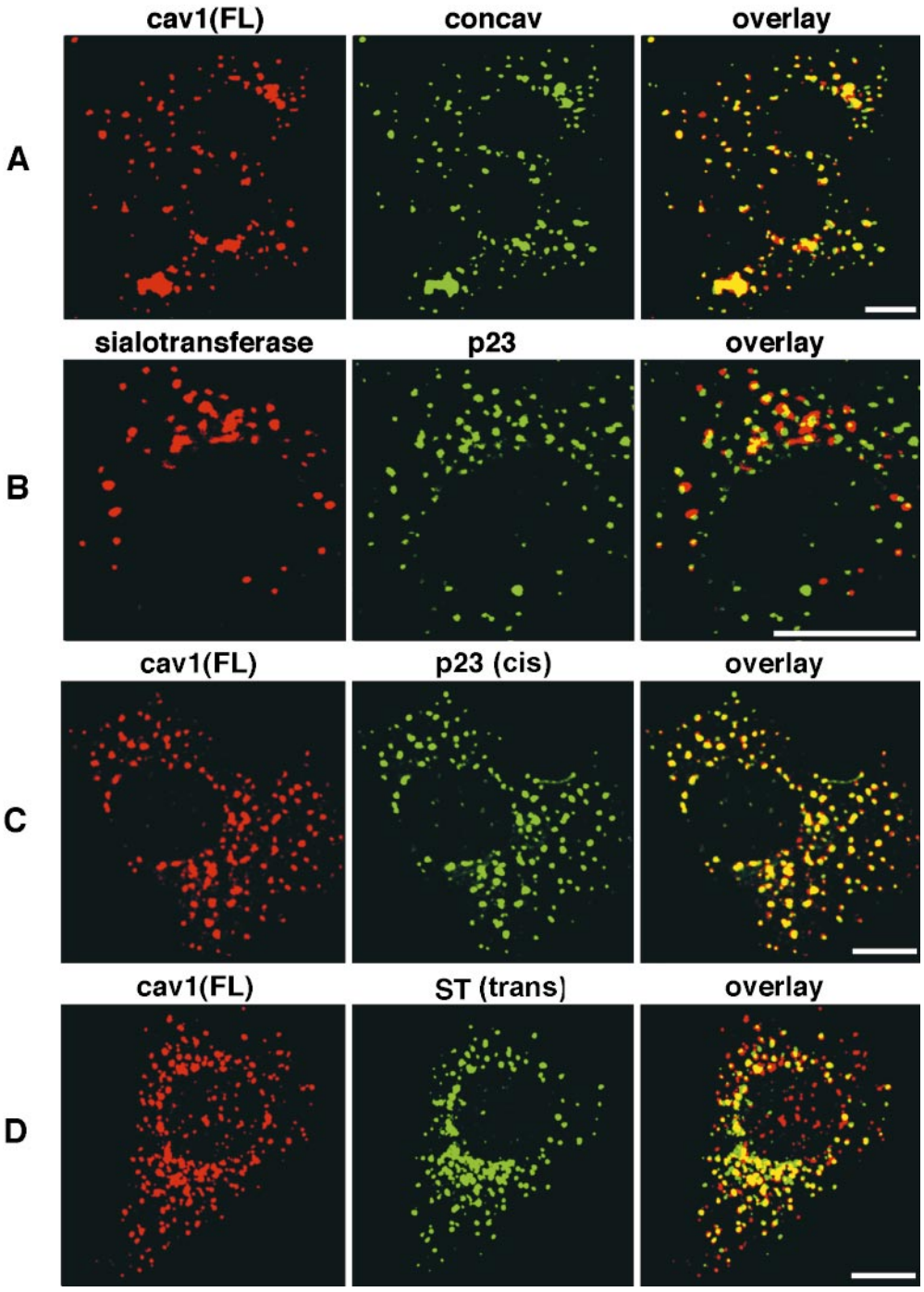

Figure 4. Immunofluorescent detection of cav-1 and Golgi markers in BHK cells after nocodazole treatment. BHK cells were treated with nocodazole to cause Golgi dispersion. (A) Cells were double labeled for endogenous caveolin using commercial monoclonal antibodies to caveolin-1 (cav1(FL)) and the affinity-purified concav antibody. The two antibodies colocalize throughout the cell. (B) The efficiency of Golgi marker separation by nocodazole was examined by comparing a cis-Golgi marker, p23, and expressed sialotransferase (B). Endogenous p23 and expressed sialotransferase were partially separated after nocodazole treatment (note fewer yellow structures and greater number of green and red dots in B overlay). (C and D) Cells were double labeled with cav-1(FL) and with p23 (C) or expressed sialotransferase (D) before examination by confocal microscopy. Note the higher degree of colocalization (indicated by the greater number of yellow dots) of caveolin with the cis marker, p23, than with the trans marker, ST. Bars, 10 μm.

Mutational Analysis of Caveolin Targeting: Targeting of an NH_2-terminal Deletion Mutant

We examined whether a specific region of the caveolin molecule is responsible for the localization of caveolin to the Golgi complex. To avoid potential problems of association with endogenous caveolins (Song et al., 1997) we prepared mutants of cav-3 which are not endogenously expressed in BHK cells. A series of cav-3 deletion mutants with a COOH-terminal HA tag were prepared (see Fig. 6 A) and expressed transiently in BHK cells. As shown in Fig. 6, C–F, the NH_2-terminal deletion mutants showed overlapping but distinct localization patterns with varying degrees of surface and intracellular labeling. Most strikingly, $Cav3^{DGV}$, which lacks the NH_2-terminal region up to the scaffolding domain (residues 54–151), showed no hint of surface labeling and this mutant was chosen for more detailed analysis. $Cav3^{DGV}$ localized to the Golgi apparatus and to punctate structures throughout the cell. This was examined in more detail by immunoelectron microscopy using antibodies to the HA tag (Fig. 7). Consistent with the confocal microscopic analysis, $Cav3^{DGV}$ was shown to associate with the Golgi complex (Fig. 7) as well as

Published June 28, 1999

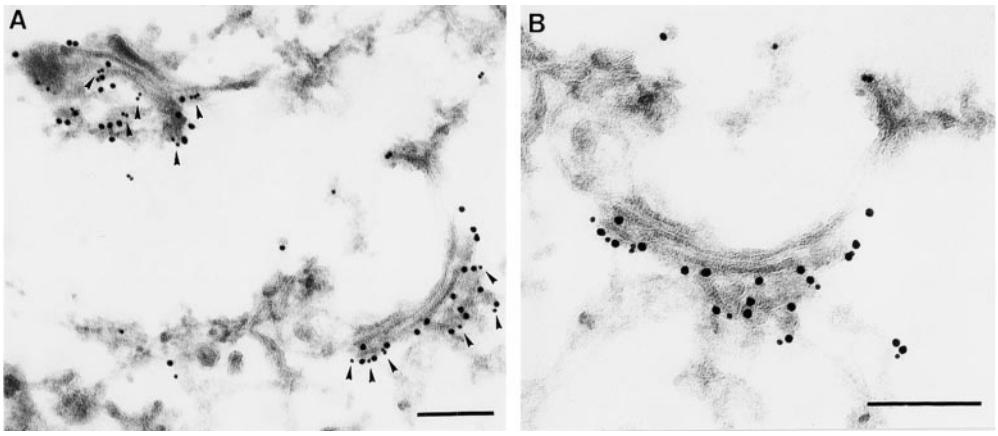

Figure 5. Immunoelectron microscopic localization of caveolin in Golgi fractions from BHK cells. Thawed cryosections of Golgi fractions prepared according to (Rojo et al., 1997) were double labeled with antibodies to p23 followed by 15 nm protein A–gold and anti-cavC followed by 10 nm protein A–gold. The two Golgi stacks show polarized labeling for p23 and for caveolin (arrowheads) as shown at higher magnification in B. Bars, 200 nm.

intracellular vesicular elements (Roy et al., 1999). The Golgi labeling colocalized with ERD2 (KDEL-receptor) showing that the protein was concentrated in the cis-Golgi complex (Fig. 7 B). In a small proportion of highly expressing cells labeling was also observed within the endoplasmic reticulum (not shown).

Targeting of a COOH-terminal Caveolin Domain

These studies suggest that Golgi targeting/retention information resides in the COOH-terminal portion of the molecule. To identify the relevant domain we expressed a construct comprising just the putative COOH-terminal cytoplasmic domain of cav-3 (residues 108–151). This domain has previously been assigned as cytoplasmically orientated based on amino acid sequence predictions, on antibody recognition of the COOH-terminal domain in permeabilized cells (Dupree et al., 1993), and in vitro import experiments (Monier et al., 1995). The construct termed Cav3^{KSY} was expressed in BHK cells with an HA epitope tag. Cav3^{KSY} was targeted specifically to the perinuclear area of the cell (Fig. 6 F). No surface staining was apparent in contrast to the full-length protein expressed under the same conditions. In very highly expressing cells a cytoplasmic staining in addition to the Golgi complex was apparent (not shown).

The specific localization of this mutant was confirmed by immunoelectron microscopy (Fig. 8). Expressing cells showed Golgi labeling for the expressed protein. No labeling was associated with the plasma membrane or other organelles. Very high expressing cells showed dispersed cytosolic staining throughout the cell in addition to the Golgi staining but unlike Cav3^{DGV}-expressing cells, Cav3^{KSY} expressing cells never showed ER staining. Together with the immunofluorescence results this suggests that the association of this caveolin fragment with the Golgi complex is a saturable process.

We then localized the Cav3^{KSY} mutant with respect to the defined Golgi markers p23, tST, and giantin (Linstedt and Hauri, 1993) at the light and electron microscopic levels. The Cav3^{KSY} colocalized with all three markers in untreated cells (Fig. 9, A–F). However, after nocodazole treatment, colocalization with cis markers was more complete than with the medial or trans Golgi markers (Fig. 10, A–I). This confirms that the localization of Cav3^{KSY} closely follows that of endogenous cav-1 and suggests that the Cav3^{KSY} is not mislocalized to an irrelevant domain. We also examined the distribution of Cav3^{KSY} at the electron microscopic level with respect to defined markers. Cav3^{KSY} showed a clear colocalization with the cis-Golgi markers p23 (Fig. 8, B and C) and with ERD2 (not shown). In extracted cells (e.g., Fig. 8 C) labeling was clearly shown to be associated with the cytoplasmic face of the membrane.

The distribution of Cav3^{KSY} with respect to endogenous caveolin was also examined. Cav3^{KSY} showed colocalization, as judged by confocal immunofluorescence microscopy, with antibodies to the COOH terminus of caveolin (Fig. 9, G and H). In contrast, as expected antibodies to the NH_2 terminus of caveolin which only label the surface caveolin, showed no colocalization with Cav3^{KSY} (not shown). A consistent observation in the Cav3^{KSY}-expressing cells was a dramatic decrease in the endogenous Golgi caveolin labeling in a subpopulation (30–40%) of expressing cells (Fig. 9, I and J). This decrease appeared unrelated to expression levels and was observed with different labeling sequences, in combination with nocodazole treatment (Fig. 9, K and L) and with the three different antibodies against caveolin which recognize different domains of the molecule. This suggests that the association of Cav3^{KSY} with the Golgi complex either decreases accessibility of caveolin antibodies to the endogenous caveolin or, more likely, decreases the Golgi-associated pool of caveolin.

Although the oligomerization of caveolin has been shown to be isotype-specific in vitro (Song et al., 1996), the possibility remained that the Golgi-association of Cav3^{KSY} could represent association with endogenous Golgi caveolin. To test this in vivo we made use of the epithelial cell line, FRT, which lacks caveolin and caveolae (Lipardi et al., 1998). Cav3^{KSY} expressed in these cells showed the characteristic staining of the Golgi complex (Fig. 11, A and B) which colocalized with p23 (not shown), strongly suggesting that the association of Cav3^{KSY} is independent of endogenous caveolin. This was further tested by double transfection of Cav3^{KSY} and wild-type cav-1 or GFP-tagged cav-3. Cav3^{KSY} colocalized with the expressed pro-

Published June 28, 1999

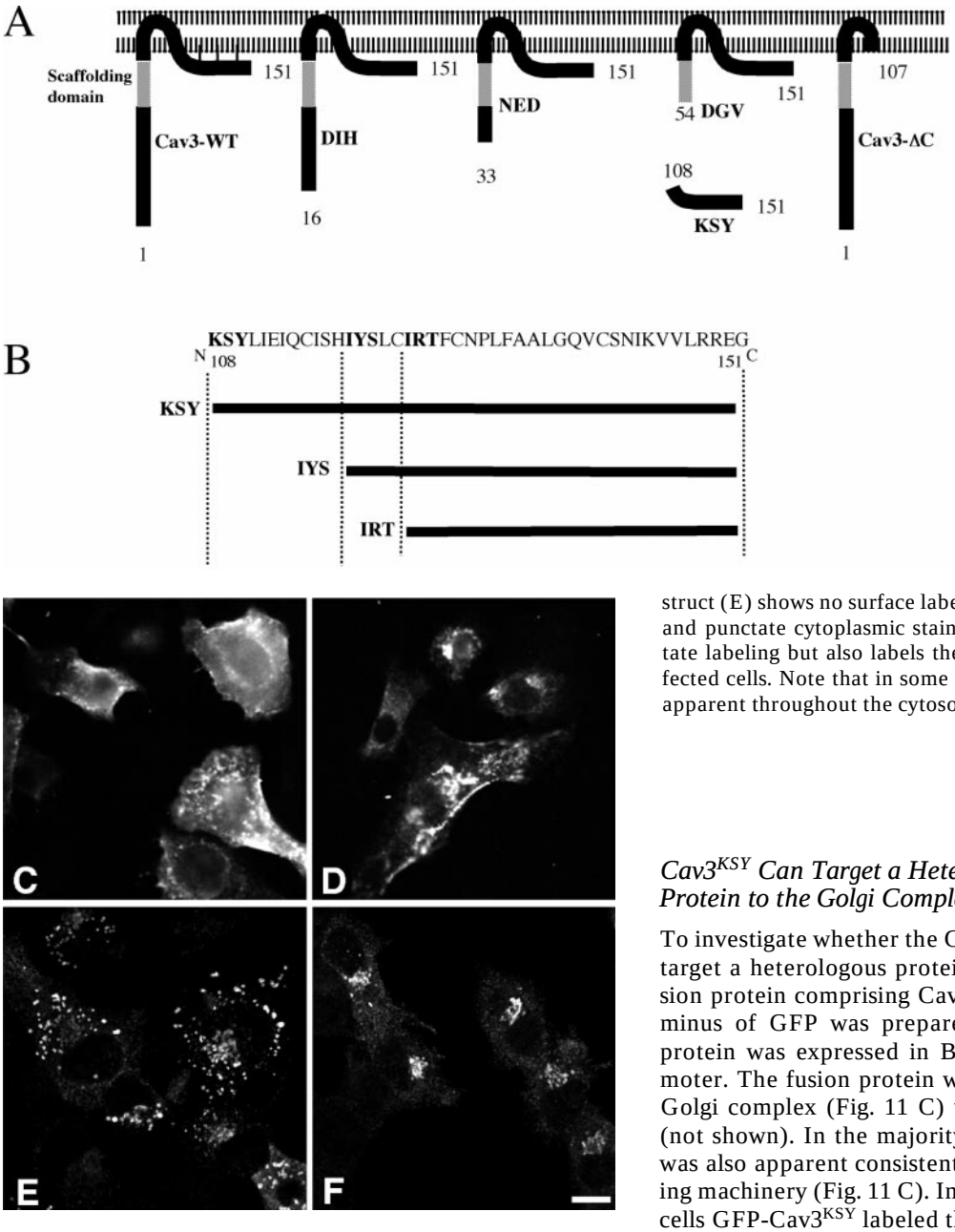

Figure 6. Diagrammatic representation and immunofluorescent detection of cav-3 mutants. (A) Summary of some of the mutants used in this study and their predicted topology. (B) Amino acid sequence of putative COOH-terminal domain of cav-3 with additional COOH-terminal mutants. (C–F) BHK cells were transfected with a series of HA-tagged caveolin-3 mutants as follows: $Cav3^{DIH}$ (panel C), $Cav3^{NED}$ (D), $Cav3^{DGV}$ (E), and $Cav3^{KSY}$ (F). They were then labeled with antibodies to the HA tag and examined by confocal microscopy. While there is clearly surface staining and internal staining in A and B, the $Cav3^{DGV}$ construct (E) shows no surface labeling but only perinuclear labeling and punctate cytoplasmic staining. $Cav3^{KSY}$ (F) lacks the punctate labeling but also labels the perinuclear region of the transfected cells. Note that in some higher expressing cells labeling is apparent throughout the cytosol. Bar, 10 μm.

teins in the Golgi complex but even after high overexpression of full-length cav-3, $Cav3^{KSY}$ was not recruited to the cell surface (not shown). To examine whether removal of the COOH terminus of Cav-3 caused a loss of Golgi localization, Cav-3ΔC with an NH_2 terminal GFP tag was expressed in BHK cells. The protein showed only a reticular staining pattern consistent with an ER localization (not shown). Although these results are consistent with a role for the COOH terminus in association of caveolin with the Golgi complex they could indicate a general perturbation of folding/oligomerization leading to lack of transport from the ER. Nevertheless our results show that the COOH-terminal cytoplasmic domain of caveolin associates in a saturable fashion with the cis-Golgi complex.

$Cav3^{KSY}$ Can Target a Heterologous Cytoplasmic Protein to the Golgi Complex

To investigate whether the COOH terminus of cav-3 could target a heterologous protein to the Golgi complex, a fusion protein comprising $Cav3^{KSY}$ fused to the COOH terminus of GFP was prepared. The GFP-$Cav3^{KSY}$ fusion protein was expressed in BHK cells under a CMV promoter. The fusion protein was specifically targeted to the Golgi complex (Fig. 11 C) where it colocalized with p23 (not shown). In the majority of cells cytoplasmic staining was also apparent consistent with saturation of the targeting machinery (Fig. 11 C). In addition, in higher expressing cells GFP-$Cav3^{KSY}$ labeled the periphery of large vesicular structures in the perinuclear area of the cell (Fig. 11 D). These experiments show that the COOH-terminal domain of cav-3 is sufficient to localize a heterologous cytosolic protein to the Golgi complex.

We carried out a preliminary characterization of the regions of the COOH-terminal cytoplasmic domain which were required for Golgi location by expressing COOH-terminal fragments as fusion proteins with GFP. A 32–amino acid segment ($Cav3^{IYS}$; see Fig. 6 B) fused to GFP showed the characteristic staining pattern of the Golgi complex (Fig. 11 E). In contrast, all cells expressing the $Cav3^{IRT}$ mutant, which lacks the first five amino acids of $Cav3^{IYS}$ (see Fig. 6 B), consistently showed dispersed labeling throughout the cell (Fig. 11 F). The observed differences between the two mutants were independent of expression level. In conclusion we have identified a unique domain of the caveolin molecule which can target a heterologous protein to a specific domain of the Golgi complex.

Published June 28, 1999

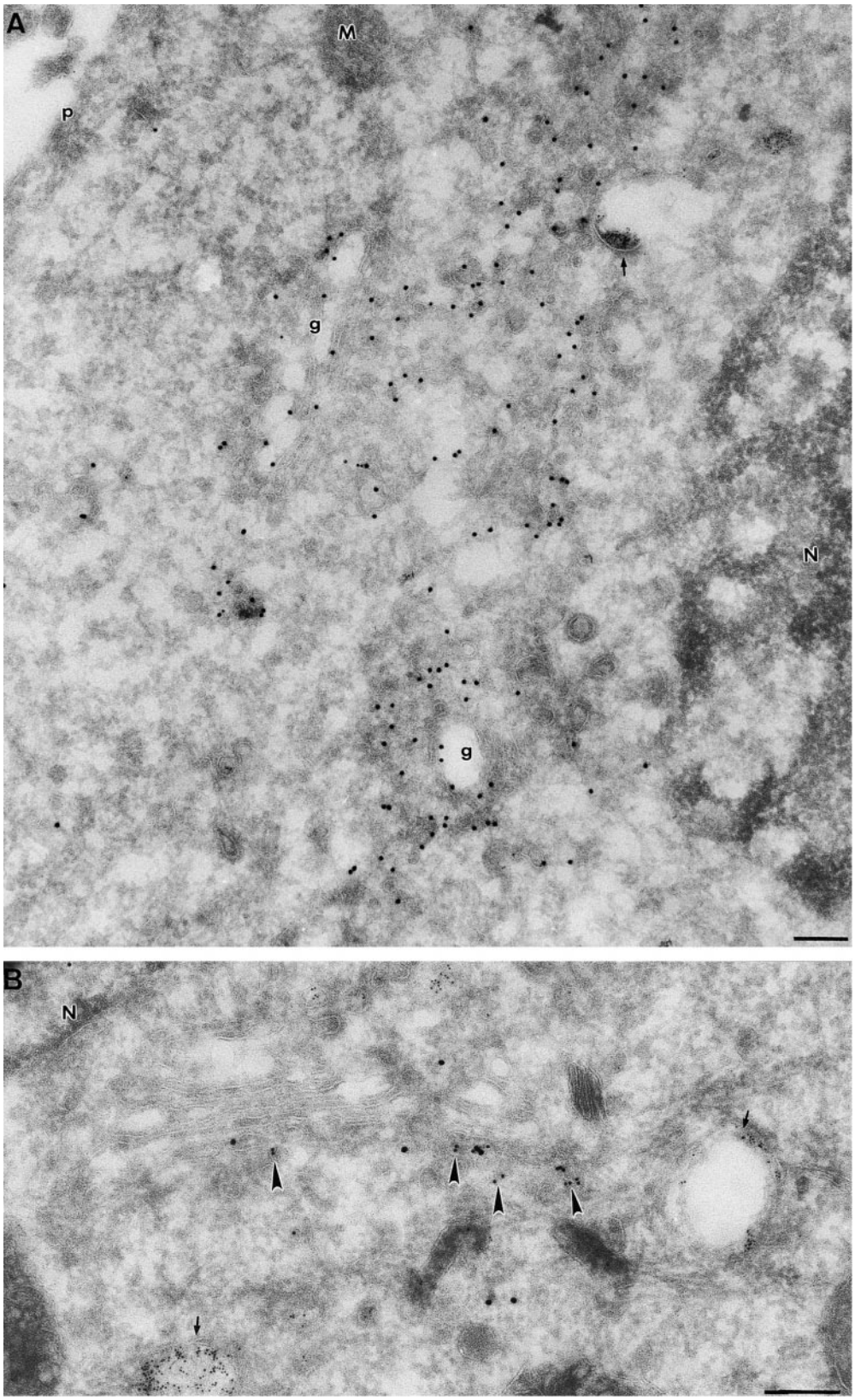

Figure 7. Immunoelectron microscopic localization of HA-tagged cav3^{DGV} in BHK cells. BHK cells were transfected with the cDNA for HA-tagged cav3^{DGV} and the overexpressed protein detected with antibodies to the HA tag. Cells were incubated with 5 nm BSA-gold for 10 min at 37°C before fixation. Thawed cryosections were labeled with antibodies to the HA tag followed by 15 nm protein A–gold. In panel B the sections were also labeled with antibodies to ERD2 followed by 10 nm protein A–gold. A shows a low magnification view of the perinuclear region of the cell showing specific labeling for the HA-tagged cav3^{DGV} in the Golgi complex (g). As shown in panel B this labeling colocalizes with the cis-Golgi marker, ERD2 (10 nm gold, arrowheads). Labeling is also associated with vesicular structures (not shown). Negligible labeling was associated with the plasma membrane (p), mitochondria (m), and early endosomes labeled by 5 nm BSA-gold (arrows). N, nucleus. Bars, 100 nm.

Caveolin COOH-terminal Constructs Show Tight Binding to Membranes: Putative Role for Palmitoylation in Golgi Association

Finally, we examined the nature of the association of Cav3^{KSY} with the Golgi complex. BHK cells expressing Cav3^{KSY} were harvested, homogenized, and separated by centrifugation into crude cytosol and membrane fractions. Membranes were initially extracted with buffer containing 1% SDS or 1% Triton X-100. Fig. 12 A shows that both these detergents extracted a peptide of ~5 kD recognized

Published June 28, 1999

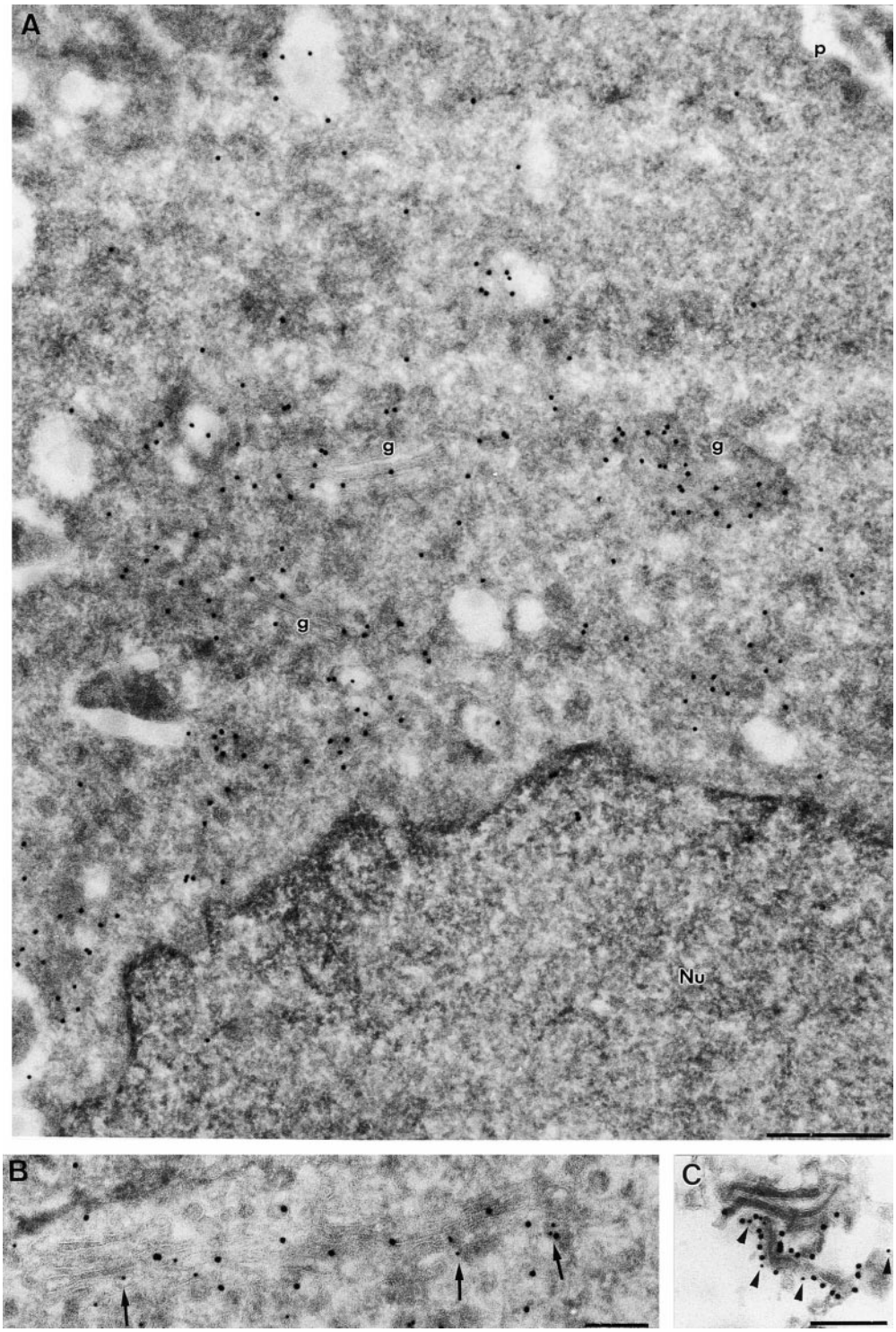

Figure 8. Immunoelectron microscopic localization of HA-tagged Cav3^{KSY} in BHK cells. BHK cells were transfected with the cDNA for HA-tagged Cav3^{KSY} and the overexpressed protein detected with antibodies to the HA tag. Thawed cryosections were labeled with antibodies to the HA tag followed by 15 nm protein A–gold. In B, the sections were also labeled with antibodies to p23 followed by 10 nm protein A–gold (arrows). In C, sections were labeled for HA with 10 nm gold (arrowheads) and p23 with 15 nm gold. A shows a low magnification view showing specific labeling for the HA-tagged cav3^{KSY} in the Golgi complex (g). As shown in B this labeling colocalizes with the cis-Golgi marker, p23 (10 nm gold). C shows the Golgi complex of an extracted cell in which the p23 labeling is greatly increased as compared with unextracted cells. The polarity of the p23 and the HA-tagged Cav3^{KSY} (arrowheads) is clearly evident. Negligible labeling was associated with the plasma membrane (p). Bars: (A) 500 nm; (B and C) 200 nm.

by the anti-HA antibody which was not present in mock transfected control cells. Treatment with either 1 M KCl or alkaline 0.1 M Na_2CO_3 both failed to extract Cav3^{KSY} from the pellet (Fig. 12 B). To confirm the apparent hydrophobicity of Cav3^{KSY} the membranes were treated with Triton X-114 which enables phase separation of amphiphilic from hydrophilic proteins. Fig. 12 C shows that Cav3^{KSY} was detected only in the amphiphilic Triton X-114 phase. We then examined the membrane association of the GFP-Cav3^{KSY} chimera. While expressed WT-GFP was predominantly in the soluble fraction, as predicted for a cytosolic protein, the majority of GFP-Cav3^{KSY} was targeted to the membrane fraction (Fig. 12 D).

Cav-1 has been shown to be palmitoylated and so we examined whether this lipid modification might be required for the Golgi localization of the COOH-terminal caveolin fragment. A full-length cav-1 construct in which the three COOH-terminal palmitoylated cysteines have been mu-

Published June 28, 1999

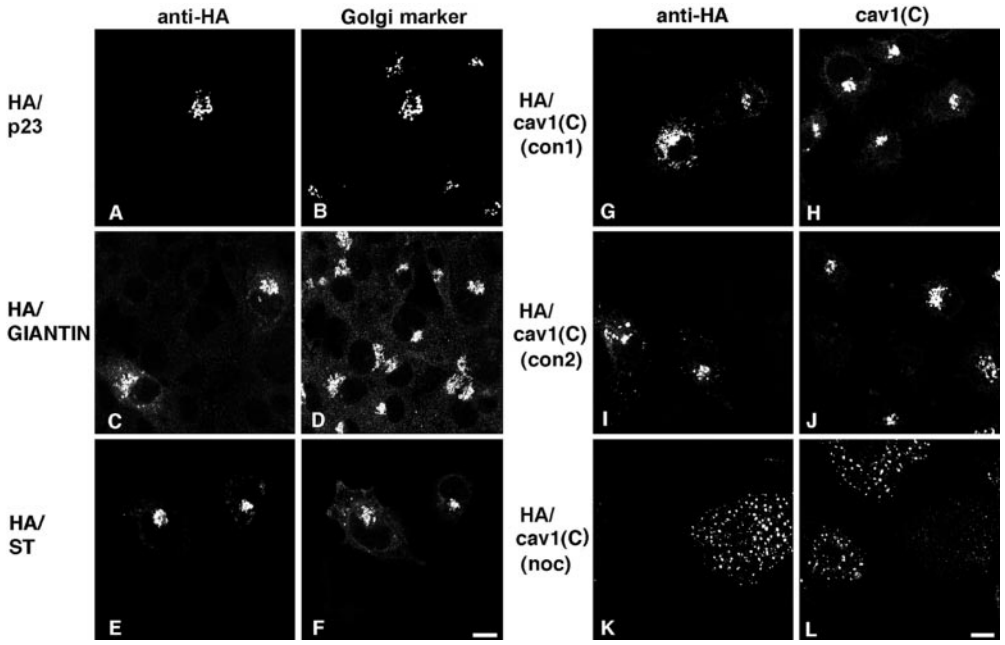

Figure 9. Colocalization of HA-tagged Cav3^{KSY} with Golgi markers and caveolin in BHK cells. Cav3^{KSY} transfected BHK cells were double-labeled with antibodies to the HA epitope (A, C, E, G, I, and K) and with antibodies against a cis-Golgi marker, p23 (B), medial-Golgi marker giantin (D), TGN marker sialotransferase (F), and caveolin (cav1C; H, J, and L). Cells were then examined by confocal microscopy. Colocalization is evident with all three Golgi markers (A–F). (G–L) Immunolocalization of HA-tagged Cav3^{KSY} and endogenous cav-1. In many cells the HA-tagged cav3^{KSY} and the caveolin colocalize (G and H). However, a consistent observation was that in many of the Cav3^{KSY} transfected cells (varying between 30 and 40%; five independent experiments) the endogenous cav-1 signal was diminished or undetectable (I and J). Treatment with nocodazole did not abrogate this signal loss (K and L). Bars, 10 μm.

tated to alanine (Cav-1Cys-Ala) has already been described and characterized (Dietzen et al., 1995; Monier et al., 1996). We used a WT cav-1 construct to generate the cav-1 equivalent of the Cav3^{KSY} (Cav-1^{KSF}) and the Cav-1Cys-Ala cDNA to generate the corresponding Cys-Ala mutant (Cav-1^{KSF}Δp). Each construct incorporated a COOH-terminal HA-tag. The constructs were expressed in BHK cells and their distribution examined by immunofluores-

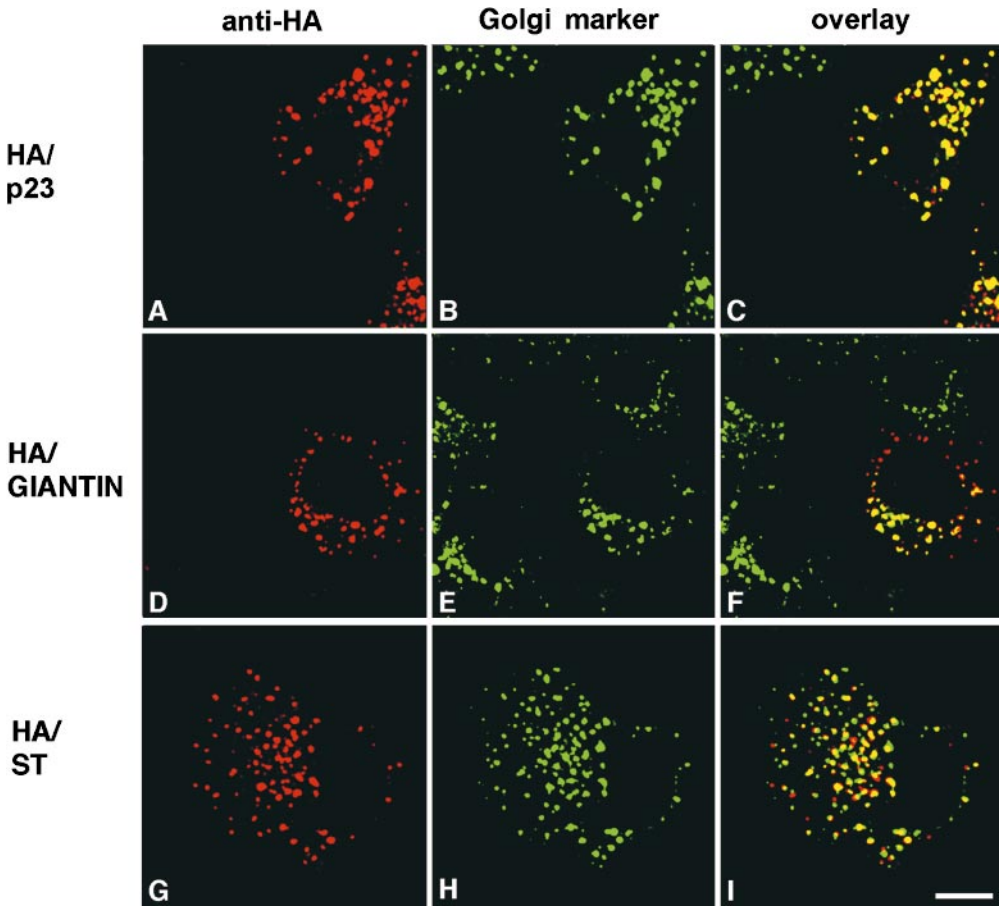

Figure 10. Immunolocalization of HA-tagged Cav3^{KSY} in transfected BHK cells treated with nocodazole to cause Golgi dispersion. BHK cells were transfected with HA-tagged Cav3^{KSY} or double transfected with HA-tagged Cav3^{KSY} and sialotransferase, and then were treated with 10 μM nocodazole for 2 h before fixation to obtain separation of Golgi markers. The cells were then double labeled with antibodies to the HA tag and with antibodies to either p23 (A–C), giantin (D–F), or epitope-tagged sialotransferase (ST; G–I). The cells were then examined by confocal microscopy. Close examination of the overlays (shown in C, F, and I) show that the colocalization of the HA tag with p23 (A–C) is more complete than with giantin (D–F) or tST (G–I) (compare the relatively high proportion of completely yellow dots in C as compared with F and more strikingly, I). Bar, 10 μm.

Published June 28, 1999

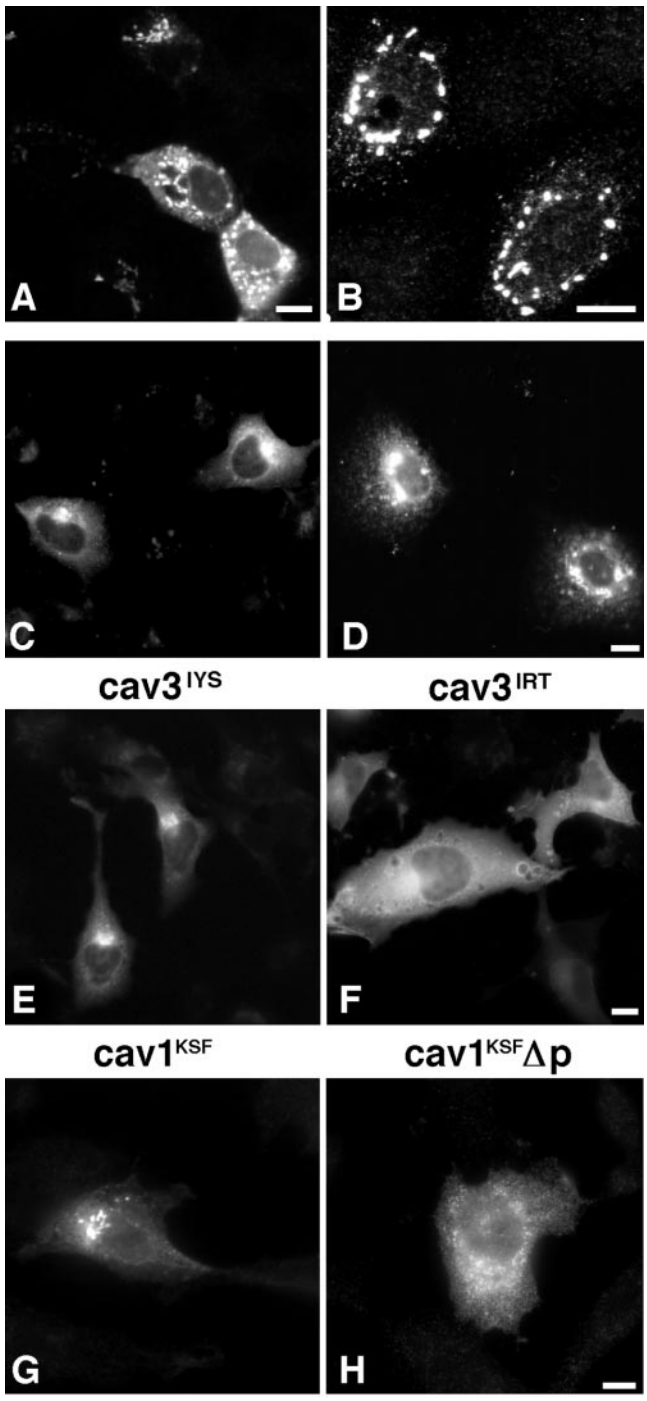

Figure 11. The COOH-terminal domain of cav-3 labels the Golgi of FRT cells and can target a cytosolic protein to the Golgi complex. (A and B) Immunofluorescence of HA-tagged Cav3^{KSY} in FRT cells. FRT cells, an epithelial cell line which expresses no endogenous caveolin, were transfected with the HA-tagged Cav3^{KSY}. While many of these cells showed HA labeling throughout the cytoplasm (A), all showed some association with perinuclear structures (B) which colocalized with p23 (not shown). (C and D) Localization of GFP-Cav3^{KSY} in transfected BHK cells. BHK cells were transfected with a GFP-Cav3^{KSY} fusion protein. The majority of expressing cells show labeling throughout the cytoplasm in addition to a clear Golgi labeling (C). In some higher expressing cells the Golgi appears to show morphological changes (D). (E–H) BHK cells were transfected with caveolin mutants as indicated and localized by confocal microscopy. (E and F) transfected Cav3^{IYS} (see Fig. 6) localizes to the Golgi complex whereas Cav3^{IRT} consistently showed a more diffuse staining, irrespective of expression levels. (G and H) Immunolocalization of Cav-1^{KSF} and the palmitoylation-deficient mutant Cav-1$^{KSF}\Delta$p. Cav-1^{KSF} generally showed a characteristic Golgi labeling pattern while those transfected with Cav-1$^{KSF}\Delta$p consistently gave a more diffuse cytoplasmic labeling. Bars, 10 μm.

cence. As expected the Cav-1^{KSF} was specifically localized to the Golgi complex consistent with the results with the cav-3 constructs (Fig. 11 G). In contrast, cells expressing Cav-1$^{KSF}\Delta$p did not show a characteristic Golgi staining (Fig. 11 H) although both Cav-1^{KSF} and Cav-1$^{KSF}\Delta$p were membrane associated as judged biochemically (not shown). These results suggest a role for palmitoylation in the specific association of the COOH terminus of caveolin with the Golgi complex.

Discussion

Crucial to understanding the role of caveolins is the determination of the exact cellular distribution and intracellular itinerary of this family of proteins. In the present study we have localized caveolin using different specific antibodies and analyzed the targeting information in the caveolin molecule. In particular, we have shown that in addition to surface caveolae, caveolin is also associated with the cis-Golgi in all cell types studied. However, different epitopes are exposed in these locations. We have then used a mutational approach to examine caveolin cycling and targeting. The NH_2 terminus of the protein was shown to be required for caveolae targeting while the COOH terminus contains a Golgi targeting motif which is sufficient to target a heterologous protein to the Golgi.

Caveolin has been shown to play an important role in signal transduction at the cell surface and many signaling molecules have been postulated to interact with caveolin directly. Upon cell transformation caveolin levels decrease (Koleske et al., 1995) and it has also been shown that caveolin is phosphorylated upon Rous sarcoma virus transformation (Glenney, 1989; Li et al., 1996b) or upon stimulation of adipocytes with insulin (Mastick et al., 1995; Mastick and Saltiel, 1997). In view of these functions, primarily assigned to the plasma membrane, it initially appears somewhat surprising that caveolin is cycling between the cell surface and intracellular compartments. In fact early studies suggested that caveolin was exclusively a surface protein based on immunofluorescence and pre-embedding immunoelectron microscopy (Rothberg et al., 1992). Other studies showed that caveolin is associated with the Golgi complex but this location was only visualized with certain antibodies (Dupree et al., 1993) or with overexpressed protein (Kurzchalia et al., 1992). This labeling was assigned to the TGN and exocytic vesicles consistent with a conventional cycling pathway between the Golgi and the cell surface. Later work outlined a quite distinct cycling pathway for the caveolin molecule involving transport of caveolin to the ER and cis-Golgi. In these studies caveolin was associated with the plasma membrane in control cells (human fibroblasts) but redistributed to intracellular compartments only upon treatment with cholesterol oxidase or

Published June 28, 1999

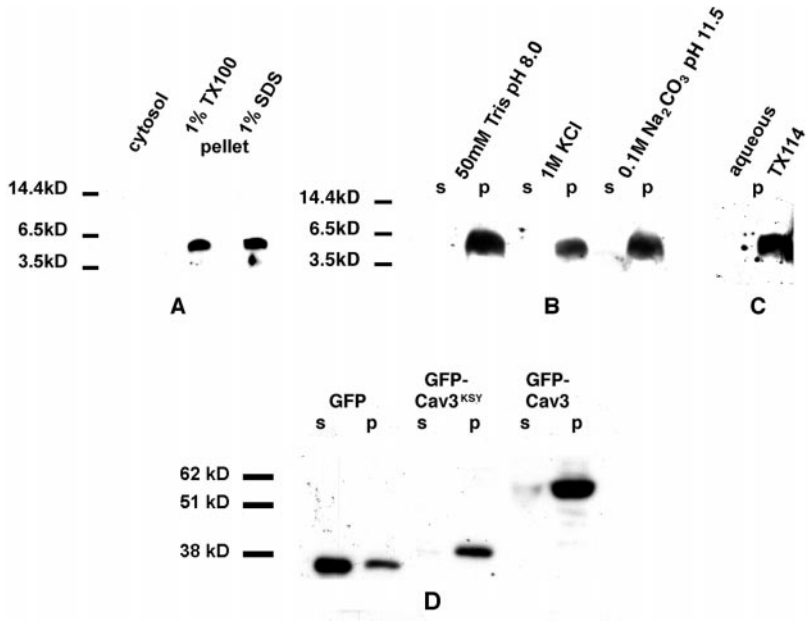

Figure 12. Biochemical characterization of Cav3^{KSY}. (A) Detergent solubility of HA tagged Cav3^{KSY}. Western blotting was used to identify the epitope tagged protein recognized by an anti-HA antibody. No significant signal was observed in the cytosol fraction. Analysis of membranes (100,000-*g* pellet) extracted with 1% Triton X-100 as well as 1% SDS shows a ~5-kD band in the transfected samples recognized by the anti-HA antibody. (B) Comparison of supernatant (s) and pellet (p) after extraction from membranes (100,000-*g* pellet) with 1 M KCl and alkaline 0.1 M Na_2CO_3 showing Cav3^{KSY} is retained in the insoluble fraction. (C) Separation of amphiphilic and hydrophilic proteins from membranes with Triton X-114 shows Cav3^{KSY} partitioning into the Triton X-114 phase. (D) Western blot with anti-GFP antibody showing the relative distributions of transfected WT-GFP, GFP-Cav3^{KSY}, and GFP-Cav3(FL) in BHK crude cytosol (s) and membrane (p) fractions.

nocodazole (Smart et al., 1994; Conrad et al., 1995). Subsequent studies have raised the possibility that the primary function of caveolin in mammalian cells is to regulate cholesterol transport (Fielding and Fielding, 1997). To understand these processes it is essential that the caveolin distribution and routing is determined and the molecular machinery defined. This study has started to address these issues and to provide tools for further analysis.

First, we have shown that in all cell types studied a pool of caveolin is present in the Golgi complex. However, our studies demonstrate some of the difficulties associated with localizing caveolin. Different antibodies clearly recognize different pools of the protein, at least as seen by immunofluorescence. Of particular interest is a new antibody, characterized here, which was raised against the scaffolding domain of the caveolin molecule. This domain is highly conserved both in evolution (Tang et al., 1997) and between different mammalian caveolins (Parton, 1996) and consistent with this we have shown that it recognizes all three mammalian caveolins. This domain interacts with a number of signaling molecules (Li et al., 1996a) and is also involved in self-association to form oligomers (Sargiacomo et al., 1995). Remarkably, despite these protein-protein interactions, the antibody gave a specific signal by immunofluorescence but only recognized the Golgi form of the protein by this technique. A similar specificity was seen with antibodies against the COOH terminus. The molecular basis for the selectivity is unclear. Oligomerization has been shown to occur early in the biosynthetic pathway immediately after cotranslational insertion into the endoplasmic reticulum. We suspect that higher order complexes of proteins and lipids might restrict antibody accessibility. In fact, in ultrathin frozen sections, antibodies against the COOH terminus or against the conserved domain do recognize surface protein suggesting that epitopes are exposed upon sectioning (results not shown). This suggests that protein–protein interactions might not be responsible for blocking accessibility. Whatever the mechanism, it is apparent that care should be taken in interpreting caveolin localization based on single antibodies.

We were also able to define the domain of the Golgi with which the caveolin is detectable as the cis-Golgi complex based on immunoelectron microscopic colocalization with defined markers. This presumably represents a pool of caveolin which cycles through the entire Golgi and TGN to the surface as cav-1 has been detected within Golgi derived exocytic vesicles (Kurzchalia et al., 1992) and is directly implicated in exocytic transport to the apical cell surface of epithelial cells (Scheiffele et al., 1998). This implies that caveolin follows an unusual cycling pathway to reach early compartments of the biosynthetic pathway, distinct from that followed by molecules such as furin and TGN38 (Chapman and Munro, 1994). In this way the results are consistent with those showing redistribution of caveolin in response to cholesterol oxidase or nocodazole (Smart et al., 1994; Conrad et al., 1995). However, our results differ significantly in other ways. Most notably, in all cell types studied including human fibroblasts as used in the above studies, caveolin is not only detectable on the surface but also in the Golgi complex under all conditions tested. The distribution of surface caveolin was unchanged by nocodazole treatment (not shown). Our subsequent experiments were designed to analyze the Golgi association of caveolin further and to determine the molecular basis of this targeting through mutational analysis of the caveolin molecule.

Mutational Analysis of Caveolin Targeting

We chose to analyze caveolin targeting using the muscle-specific caveolin isoform, cav-3, expressed in BHK cells. The first striking observation was that truncation mutants lacking the first 54 amino acids no longer associated with surface caveolae as determined by immunofluorescence and immunoelectron microscopy with (COOH-terminal) epitope-tagged constructs and with the (NH_2-terminally)

Published June 28, 1999

GFP-tagged fusion protein. In contrast, the removal of the first 33 amino acids had no effect on surface localization. This may indicate that residues 33–54 are required for caveolae targeting or retention or at least implies that removal of the first 54 amino acids disrupts this process. Expression of the entire NH_2 terminus produced a soluble protein with no detectable association with membranes (results not shown).

We then went on to analyze the domains of the caveolin molecule required for Golgi association. Removal of the NH_2 terminus had no effect on Golgi localization of the protein. Therefore, we investigated whether the COOH terminus contains Golgi targeting information. Surprisingly, the putative COOH-terminal domain associated with the cis-Golgi even when expressed alone, presumably as a soluble protein. Moreover, this domain was able to target a heterologous soluble protein, GFP, to the Golgi. It is important to note that GFP was fused to the NH_2 terminus of the construct, in place of the putative intramembrane domain. The domain required for targeting GFP to the Golgi was narrowed down to a relatively hydrophobic region of 32 amino acids of which the first five amino acids were essential. This region showed no significant homology with other Golgi associated proteins in amino acid sequence. This small domain is sufficient for Golgi targeting and although normally part of a membrane protein can apparently function in the context of a soluble protein. This property may not be so surprising in view of recent reports that caveolin is not always an integral membrane protein but can exist in a cytosolic complex with cholesterol and chaperones (Uittenbogaard et al., 1998). Our morphological studies suggest that association with the Golgi complex is a saturable process as higher expressing cells showed labeling throughout the cell by both immunofluorescence (particularly with the GFP-tagged construct) and by immunoelectron microscopy.

What is the molecular basis of the association with the Golgi complex? Our studies show that the protein does not associate with endogenous caveolins consistent with in vitro studies of caveolin oligomer formation (Song et al., 1997). The caveolin COOH terminus may therefore interact with a specific Golgi component. Our biochemical studies showed a surprisingly tight association with the membrane. Detergent treatment, but not high pH sodium carbonate, released the GFP-$Cav3^{KSY}$ fusion protein from membranes. One possibility is that like cav-1 (Dietzen et al., 1995; Monier et al., 1996), cav-3 is palmitoylated and this modification is involved in Golgi membrane association. Indeed, we showed that the corresponding domain of cav-1 also associates preferentially with the Golgi complex and that this specific localization is lost upon modification of the three COOH-terminal cysteines to alanines. These three cysteine residues have been shown to be palmitoylated in vivo and to play a role in stabilization of higher order oligomers (Monier et al., 1996) but not to play a role in targeting to caveolae (Dietzen et al., 1995; Monier et al., 1996; Parton, R., and T. Kurzchalia, unpublished observation). Cav-1 can be palmitoylated on all three cysteine residues within the COOH terminus (Monier et al., 1996). While palmitoylation alone is unable to mediate specific association with the Golgi, the lipid modification may contribute to the tight association with the Golgi membrane in combination with protein interactions. It is interesting to note that a number of other Golgi proteins are palmitoylated such as the glutamic acid decarboxylase isoform, GAD65 (Solimena et al., 1994; Dirkx et al., 1995), and eNOS (Sessa et al., 1995; Liu et al., 1997) but palmitoylation is not required for the Golgi association. Interestingly, eNOS cycles between surface caveolae and the Golgi complex and shows a functional interaction with caveolin (Michel et al., 1997; Feron et al., 1998). Palmitoylation has been implicated in the lateral segregation of membrane associated proteins into DIGs (see Introduction) but, unlike the full-length caveolins, $Cav3^{KSY}$ is detergent soluble (results not shown). As detergent insolubility is acquired in the late Golgi/TGN (Scheiffele et al., 1998) this is consistent with the proposed cis-Golgi location.

As well as protein interactions it is possible that the Golgi association of $Cav3^{KSY}$ relies on specific lipid interactions. Recently it was demonstrated that the cytoplasmic oxysterol-binding protein, which associates with the Golgi complex in response to oxysterols, is targeted specifically to this compartment through interactions with a phosphatidylinositol polyphosphate plus some other Golgi determinant (Levine and Munro, 1998). The COOH-terminal Golgi targeted fragment of caveolin is relatively hydrophobic and secondary structure predictions show a possible helical conformation but it appears unlikely that this domain can insert into the Golgi membrane. Previous studies have shown that a fusion protein containing the COOH terminus of cav-1 does not associate with membranes after synthesis in vitro (Monier et al., 1995). This domain of cav-1 is also accessible in vivo as COOH-terminal antibodies specifically recognize the Golgi caveolin in non-detergent permeabilized cells (Dupree et al., 1993). It has also been shown to interact in vitro with signaling molecules such as n-NOS and c-src (Venema et al., 1997). Whatever the molecular mechanism, our experiments show a striking specificity of this domain for the Golgi complex and should provide powerful tools for further analysis of the molecular basis of Golgi localization. In addition, the KSY and DGV mutants described here have functional effects on caveolae-mediated events including infection by Simian Virus 40 and Ras signaling (Roy et al., 1999). Interestingly, the present study showed that expression of the COOH-terminal mutant caused a striking loss of detectable caveolin in the Golgi region but only in some cells in the population. This effect was not correlated with expression levels and so the reason for the apparent cell-cell variation is unclear. One possibility is a difference in caveolin cycling in cells at different stages of the cell cycle.

The data presented here provide important new insights into the localization and targeting of this important class of proteins which should be taken into account in future models of caveolin function. Mutational dissection of the caveolin molecule appears to be a particularly powerful approach to gain insights into the function and dynamics of caveolin proteins and more detailed mutational studies should provide further clues into the complex and dynamic machinery comprising the caveolae membrane system.

We wish to thank David James and Jean Gruenberg for numerous discussions throughout the course of this work and for critical reading of the manuscript. We would also like to thank Tommy Nilsson for cDNA con-

structs and epitope-tag antibodies; Jean Gruenberg and Manuel Rojo for providing membrane fractions and antibodies; and Elina Ikonen for providing the recombinant cav-2-Semliki Forest Virus construct. Special thanks are due to Colin Macqueen for his help with the light microscopy.

This work was supported by grants from the National Health and Medical Research Council of Australia. The Centre for Molecular and Cellular Biology is a Special Research Centre of the Australian Research Council.

Received for publication 4 January 1999 and in revised form 26 April 1999.

References

Anderson, R.G. 1998. The caveolae membrane system. *Annu. Rev. Biochem.* 67:199–225.

Anderson, R.G.W. 1993. Plasmalemmal caveolae and GPI-anchored proteins. *Curr. Opin. Cell Biol.* 5:647–652.

Anderson, H.A., Y. Chen, and L.C. Norkin. 1996. Bound simian virus 40 translocates to caveolin-enriched membrane domains, and its entry is inhibited by drugs that selectively disrupt caveolae. *Mol. Biol. Cell.* 7:1825–1834.

Bist, A., P.E. Fielding, and C.J. Fielding. 1997. Two sterol regulatory element-like sequences mediate up-regulation of caveolin gene transcription in response to low density lipoprotein free cholesterol. *Proc. Natl. Acad. Sci. USA.* 94:10693–10698.

Bordier, C. 1981. Phase separation of integral membrane proteins in Triton X-114 solution. *J. Biol. Chem.* 256:1604–1607.

Chapman, R.E., and S. Munro. 1994. Retrieval of trans Golgi network proteins from the cell surface requires endosomal acidification. *EMBO (Eur. Mol. Biol. Organ.) J.* 13:2305–2312.

Chavrier, P., R.G. Parton, H.P. Hauri, K. Simons, and M. Zerial. 1990. Localization of low molecular weight GTP binding proteins to exocytic and endocytic compartments. *Cell.* 62:317–329.

Conrad, P.A., E.J. Smart, Y.S. Ying, R.G. Anderson, and G.S. Bloom. 1995. Caveolin cycles between plasma membrane caveolae and the Golgi complex by microtubule-dependent and microtubule-independent steps. *J. Cell Biol.* 131:1421–1433.

Dietzen, D.J., W.R. Hastings, and D.M. Lublin. 1995. Caveolin is palmitoylated on multiple cysteine residues. Palmitoylation is not necessary for localization of caveolin to caveolae. *J. Biol. Chem.* 270:6838–6842.

Dirkx, R., Jr., A. Thomas, L. Li, A. Lernmark, R.S. Sherwin, P. De Camilli, and M. Solimena. 1995. Targeting of the 67-kDa isoform of glutamic acid decarboxylase to intracellular organelles is mediated by its interaction with the NH_2-terminal region of the 65-kDa isoform of glutamic acid decarboxylase. *J. Biol. Chem.* 270:2241–2246.

Dupree, P., R.G. Parton, G. Raposo, T.V. Kurzchalia, and K. Simons. 1993. Caveolae and sorting in the trans-Golgi network of epithelial cells. *EMBO (Eur. Mol. Biol. Organ.) J.* 12:1597–1605.

Feron, O., J.B. Michel, K. Sase, and T. Michel. 1998. Dynamic regulation of endothelial nitric oxide synthase: complementary roles of dual acylation and caveolin interactions. *Biochemistry.* 37:193–200.

Fielding, P.E., and C.J. Fielding. 1995. Plasma membrane caveolae mediate the efflux of cellular free cholesterol. *Biochemistry.* 34:14288–14292.

Fielding, C.J., and P.E. Fielding. 1997. Intracellular cholesterol transport. *J. Lipid Res.* 38:1503–1521.

Fielding, C.J., A. Bist, and P.E. Fielding. 1997. Caveolin mRNA levels are up-regulated by free cholesterol and down-regulated by oxysterols in fibroblast monolayers. *Proc. Natl. Acad. Sci. USA.* 94:3753–3758.

Fra, A.M., M. Masserini, P. Palestini, S. Sonnino, and K. Simons. 1995a. A photo-reactive derivative of ganglioside GM1 specifically cross-links VIP21-caveolin on the cell surface. *FEBS Lett.* 375:11–14.

Fra, A.M., E. Williamson, K. Simons, and R.G. Parton. 1994. Detergent-insoluble glycolipid microdomains in lymphocytes in the absence of caveolae. *J. Biol. Chem.* 269:30745–30748.

Fra, A.M., E. Williamson, K. Simons, and R.G. Parton. 1995b. De novo formation of caveolae in lymphocytes by expression of VIP21-caveolin. *Proc. Natl. Acad. Sci. USA.* 92:8655–8659.

Glenney, J.R. 1989. Tyrosine phosphorylation of a 22-kDa protein is correlated with phosphorylation by Rous sarcoma virus. *J. Biol. Chem.* 264:20163–20166.

Glenney, J.J., and D. Soppet. 1992. Sequence and expression of caveolin, a protein component of caveolae plasma membrane domains phosphorylated on tyrosine in Rous sarcoma virus-transformed fibroblasts. *Proc. Natl. Acad. Sci. USA.* 89:10517–10521.

Gorodinsky, A., and D.A. Harris. 1995. Glycolipid-anchored proteins in neuroblastoma cells form detergent-resistant complexes without caveolin. *J. Cell Biol.* 129:619–627.

Griffiths, G., M. Ericsson, J. Krijnse-Locker, T. Nilsson, B. Goud, H.D. Soling, B.L. Tang, S.H. Wong, and W. Hong. 1994. Localization of the Lys, Asp, Glu, Leu tetrapeptide receptor to the Golgi complex and the intermediate compartment in mammalian cells. *J. Cell Biol.* 127:1557–1574.

Gruenberg, J., G. Griffiths, and K.E. Howell. 1989. Characterization of the early endosome and putative endocytic carrier vesicles in vivo and with an assay of vesicle function *in vitro*. *J. Cell Biol.* 108:1301–1316.

Hailstones, D., L.S. Sleer, R.G. Parton, and K.K. Stanley. 1998. Regulation of caveolin and caveolae by cholesterol in MDCK cells. *J. Lipid Res.* 39:369–379.

Keller, P., and K. Simons. 1998. Cholesterol is required for surface transport of influenza virus hemagglutinin. *J. Cell Biol.* 140:1357–1367.

Kobayashi, T., E. Stang, P. de Moerloose, R.G. Parton, and J. Gruenberg. 1998. A lipid antigen associated with the anti-phospholipid syndrome regulates endosome structure/function. *Nature.* 392:193–197.

Koleske, A.J., D. Baltimore, and M.P. Lisanti. 1995. Reduction of caveolin and caveolae in oncogenically transformed cells. *Proc. Natl. Acad. Sci. USA.* 92: 1381–1385.

Kreis, T. 1990. Role of microtubules in the organisation of the Golgi apparatus. *Cell Motil. Cytoskel.* 15:67–70.

Kurzchalia, T.V., P. Dupree, R.G. Parton, R. Kellner, H. Virta, M. Lehnert, and K. Simons. 1992. VIP21, a 21-kD membrane protein is an integral component of trans-Golgi network-derived transport vesicles. *J. Cell Biol.* 118: 1003–1014.

Levine, T.P., and S. Munro. 1998. The pleckstrin homology domain of oxysterol-binding protein recognises a determinant specific to Golgi membranes. *Curr. Biol.* 8:729–739.

Li, S., T. Okamoto, M. Chun, M. Sargiacomo, J.E. Casanova, S.H. Hansen, I. Nishimoto, and M.P. Lisanti. 1995. Evidence for a regulated interaction between heterotrimeric G proteins and caveolin. *J. Biol. Chem.* 270:15693–15701.

Li, S., J. Couet, and M.P. Lisanti. 1996a. Src tyrosine kinases, Galpha subunits, and H-Ras share a common membrane-anchored scaffolding protein, caveolin. Caveolin binding negatively regulates the auto-activation of Src tyrosine kinases. *J. Biol. Chem.* 271:29182–29190.

Li, S., R. Seitz, and M.P. Lisanti. 1996b. Phosphorylation of caveolin by Src tyrosine kinases. The alpha-isoform of caveolin is selectively phosphorylated by v-Src *in vivo*. *J. Biol. Chem.* 271:3863–3868.

Liljestrom, P., and H. Garoff. 1991. A new generation of animal cell expression vectors based on the semliki forest virus replicon. *Biotechnology.* 9:1356–1361.

Linstedt, A.D., and H.P. Hauri. 1993. Giantin, a novel conserved Golgi membrane protein containing a cytoplasmic domain of at least 350 kDa. *Mol. Biol. Cell.* 4:679–693.

Lipardi, C., R. Mora, V. Colomer, S. Paladino, L. Nitsch, E. Rodriguez-Boulan, and C. Zurzolo. 1998. Caveolin transfection results in caveolae formation but not apical sorting of glycosylphosphatidylinositol (GPI)-anchored proteins in epithelial cells. *J. Cell Biol.* 140:617–626.

Lisanti, M.P., Z. Tang, P.E. Scherer, E. Kubler, A.J. Koleske, and M. Sargiacomo. 1995. Caveolae, transmembrane signaling and cellular transformation. *Mol. Membr. Biol.* 12:121–124.

Liu, J., T.E. Hughes, and W.C. Sessa. 1997. The first 35 amino acids and fatty acylation sites determine the molecular targeting of endothelial nitric oxide synthase into the Golgi region of cells: a green fluorescent protein study. *J. Cell Biol.* 137:1525–1535.

Mastick, C.C., M.J. Brady, and A.R. Saltiel. 1995. Insulin stimulates the tyrosine phosphorylation of caveolin. *J. Cell Biol.* 129:1523–1531.

Mastick, C.C., and A.R. Saltiel. 1997. Insulin-stimulated tyrosine phosphorylation of caveolin is specific for the differentiated adipocyte phenotype in 3T3-L1 cells. *J. Biol. Chem.* 272:20706–20714.

Michel, J.B., O. Feron, K. Sase, P. Prabhakar, and T. Michel. 1997. Caveolin versus calmodulin. Counterbalancing allosteric modulators of endothelial nitric oxide synthase. *J. Biol. Chem.* 272:25907–25912.

Monier, S., D.J. Dietzen, W.R. Hastings, D.M. Lublin, and T.V. Kurzchalia. 1996. Oligomerization of VIP21-caveolin *in vitro* is stabilized by long chain fatty acylation or cholesterol. *FEBS Lett.* 388:143–149.

Monier, S., R.G. Parton, F. Vogel, J. Behlke, A. Henske, and T.V. Kurzchalia. 1995. VIP21-caveolin, a membrane protein constituent of the caveolar coat, oligomerizes *in vivo* and *in vitro*. *Mol. Biol. Cell.* 6:911–927.

Montesano, R., J. Roth, A. Robert, and L. Orci. 1982. Non-coated membrane invaginations are involved in binding and internalization of cholera and tetanus toxins. *Nature.* 296:651–653.

Murata, M., J. Peranen, R. Schreiner, F. Wieland, T.V. Kurzchalia, and K. Simons. 1995. VIP21/caveolin is a cholesterol-binding protein. *Proc. Natl. Acad. Sci. USA.* 92:10339–10343.

Okamoto, T., A. Schlegel, P.E. Scherer, and M.P. Lisanti. 1998. Caveolins, a family of scaffolding proteins for organizing "preassembled signaling complexes" at the plasma membrane. *J. Biol. Chem.* 273:5419–5422.

Olkkonen, V.M., P. Liljestrom, H. Garoff, K. Simons, and C.G. Dotti. 1993. Expression of heterologous proteins in cultured rat hippocampal neurons using the Semliki Forest virus vector. *J. Neurosci. Res.* 35:445–451.

Palade, G.E. 1953. Fine structure of blood capillaries. *J. Appl. Physics.* 24:1424.

Parton, R.G. 1996. Caveolae and caveolins. *Curr. Opin. Cell Biol.* 8:542–548.

Parton, R.G., and K. Simons. 1995. Digging into caveolae. *Science.* 269:1398–1399.

Parton, R.G., and M.R. Lindsay. 1999. Exploitation of Major Histocompatibility class I molecules and caveolae by simian virus 40. *Immunol. Rev.* In press.

Parton, R.G., B. Joggerst, and K. Simons. 1994. Regulated internalization of caveolae. *J. Cell Biol.* 127:1199–1215.

Parton, R.G., M. Way, N. Zorzi, and E. Stang. 1997. Caveolin-3 associates with developing T-tubules during muscle differentiation. *J. Cell Biol.* 136:137–154.

Rabouille, C., N. Hui, F. Hunte, R. Kieckbusch, E.G. Berger, G. Warren, and

T. Nilsson. 1995. Mapping the distribution of Golgi enzymes involved in the construction of complex oligosaccharides. *J. Cell Sci.* 108:1617–1627.

Rizzuto, R., M. Brini, P. Pizzo, M. Murgia, and T. Pozzan. 1995. Chimeric green fluorescent protein as a tool for visualizing subcellular organelles in living cells. *Curr. Biol.* 5:635–642.

Rojo, M., R. Pepperkok, G. Emery, R. Kellner, E. Stang, R.G. Parton, and J. Gruenberg. 1997. Involvement of the transmembrane protein p23 in biosynthetic protein transport. *J. Cell Biol.* 139:1119–1135.

Rothberg, K., J.E. Heuser, W.C. Donzell, Y.-S. Ying, J.R. Glenney, and R.G.W. Anderson. 1992. Caveolin, a protein component of caveolae membrane coats. *Cell.* 68:673–682.

Roy, S., R. Luetterforst, A. Harding, A. Apolloni, M. Etheridge, E. Stang, B. Rolls, J.F. Hancock, and R.G. Parton. 1999. Dominant negative caveolin selectively inhibits H-ras function by disrupting cholesterol-rich domains. *Nat. Cell Biol.* 1:98–105.

Sargiacomo, M., P.E. Scherer, Z. Tang, E. Kubler, K.S. Song, M.C. Sanders, and M.P. Lisanti. 1995. Oligomeric structure of caveolin: implications for caveolae membrane organization. *Proc. Natl. Acad. Sci. USA*. 92:9407–9411.

Scheiffele, P., P. Verkade, A.M. Fra, H. Virta, K. Simons, and E. Ikonen. 1998. Caveolin-1 and -2 in the exocytic pathway of MDCK cells. *J. Cell Biol.* 140: 795–806.

Scherer, P.E., T. Okamoto, M. Chun, I. Nishimoto, H.F. Lodish, and M.P. Lisanti. 1996. Identification, sequence, and expression of caveolin-2 defines a caveolin gene family. *Proc. Natl. Acad. Sci. USA*. 93:131–135.

Schnitzer, J.E., P. Oh, E. Pinney, and J. Allard. 1994. Filipin-sensitive caveolae-mediated transport in endothelium: reduced transcytosis, scavenger endocytosis, and capillary permeability of select macromolecules. *J. Cell Biol.* 127: 1217–1232.

Sessa, W.C., G. Garcia-Cardena, J. Liu, A. Keh, J.S. Pollock, J. Bradley, S. Thiru, I.M. Braverman, and K.M. Desai. 1995. The Golgi association of endothelial nitric oxide synthase is necessary for the efficient synthesis of nitric oxide. *J. Biol. Chem*. 270:17641–17644.

Severs, N.J. 1988. Caveolae: static inpocketings of the plasma membrane, dynamic vesicles or plain artifact? *J. Cell Sci.* 90:341–348.

Simionescu, M., and N. Simionescu. 1991. Endothelial transport of macromolecules: transcytosis and endocytosis. *Cell Biol. Rev*. 25:1–80.

Simons, K., and E. Ikonen. 1997. Functional rafts in cell membranes. *Nature.* 387:569–572.

Smart, E.J., Y.S. Ying, P.A. Conrad, and R.G. Anderson. 1994. Caveolin moves from caveolae to the Golgi apparatus in response to cholesterol oxidation. *J. Cell Biol.* 127:1185–1197.

Smart, E.J., Y. Ying, W.C. Donzell, and R.G. Anderson. 1996. A role for caveolin in transport of cholesterol from endoplasmic reticulum to plasma membrane. *J. Biol. Chem*. 271:29427–29435.

Solimena, M., R. Dirkx, Jr., M. Radzynski, O. Mundigl, and P. De Camilli. 1994. A signal located within amino acids 1-27 of GAD65 is required for its targeting to the Golgi complex region. *J. Cell Biol.* 126:331–341.

Song, S.K., S. Li, T. Okamoto, L.A. Quilliam, M. Sargiacomo, and M.P. Lisanti. 1996. Co-purification and direct interaction of Ras with caveolin, an integral membrane protein of caveolae microdomains. Detergent-free purification of caveolae microdomains. *J. Biol. Chem*. 271:9690–9697.

Song, K.S., Z. Tang, S. Li, and M.P. Lisanti. 1997. Mutational analysis of the properties of caveolin-1. A novel role for the C-terminal domain in mediating homo-typic caveolin-caveolin interactions. *J. Biol. Chem*. 272:4398–4403.

Stang, E., J. Kartenbeck, and R.G. Parton. 1997. Major histocompatibility complex class I molecules mediate association of SV40 with caveolae. *Mol. Biol. Cell.* 8:47–57.

Tang, Z., P.E. Scherer, T. Okamoto, K. Song, C. Chu, D.S. Kohtz, I. Nishimoto, H.F. Lodish, and M.P. Lisanti. 1996. Molecular cloning of caveolin–3, a novel member of the caveolin gene family expressed predominantly in muscle. *J. Biol. Chem*. 271:2255–2261.

Tang, Z., T. Okamoto, P. Boontrakulpoontawee, T. Katada, A.J. Otsuka, and M.P. Lisanti. 1997. Identification, sequence, and expression of an invertebrate caveolin gene family from the nematode *Caenorhabditis elegans*. Implications for the molecular evolution of mammalian caveolin genes. *J. Biol. Chem*. 272:2437–2445.

Tran, D., J.-L. Carpentier, F. Sawano, P. Gorden, and L. Orci. 1987. Ligands internalized through coated or non-coated invaginations follow a common intracellular pathway. *Proc. Natl. Acad. Sci. USA*. 84:7957–7961.

Uittenbogaard, A., Y. Ying, and E.J. Smart. 1998. Characterization of a cytosolic heat-shock protein-caveolin chaperone complex. Involvement in cholesterol trafficking. *J. Biol. Chem*. 273:6525–6532.

Ullrich, O., S. Reinsch, S. Urbé, M. Zerial, and R.G. Parton. 1996. Rab11 regulates recycling through the pericentriolar recycling endosome. 135:913–924.

Venema, V.J., H. Ju, R. Zou, and R.C. Venema. 1997. Interaction of neuronal nitric-oxide synthase with caveolin-3 in skeletal muscle. Identification of a novel caveolin scaffolding/inhibitory domain. *J. Biol. Chem*. 272:28187–28190.

Way, M., and R.G. Parton. 1995. M-caveolin, a muscle-specific caveolin-related protein. *FEBS Lett.* 376:108–112.

Yamada, E. 1955. The fine structure of the gall bladder epithelium of the mouse. *J. Biophys. Biochem. Cytol.* 1:445–458.